NASA TECHNICAL NOTE

NASA TN D-6053

c. 1

NASA TN D-6053

FLIGHT EVALUATION OF GROUND EFFECT ON SEVERAL LOW-ASPECT-RATIO AIRPLANES

by Paul A. Baker, William G. Schweikhard, and William R. Young

Flight Research Center
Edwards, Calif. 93523

NATIONAL AERONAUTICS AND SPACE ADMINISTRATION • WASHINGTON, D. C. • OCTOBER 1970

1. Report No. NASA TN D-6053	2. Government Accession No.	3. Recipient's Catalog No.
4. Title and Subtitle FLIGHT EVALUATION OF GROUND EFFECT ON SEVERAL LOW-ASPECT-RATIO AIRPLANES		5. Report Date October 1970 6. Performing Organization Code
7. Author(s) Paul A. Baker, William G. Schweikhard, and William R. Young		8. Performing Organization Report No. H-550 10. Work Unit No. 126-62-03-02-24
9. Performing Organization Name and Address NASA Flight Research Center P. O. Box 273 Edwards, California 93523		11. Contract or Grant No. 13. Type of Report and Period Covered Technical Note
12. Sponsoring Agency Name and Address National Aeronautics and Space Administration Washington, D. C. 20546		14. Sponsoring Agency Code

15. Supplementary Notes

16. Abstract

A constant-angle-of-attack-approach technique was used to measure ground effect on several low-aspect-ratio aircraft. The flight results were compared with results from constant-altitude flybys, wind-tunnel studies, and theoretical prediction data. It was found that the constant-angle-of-attack technique provided data that were consistent with data obtained from constant-altitude flybys and required fewer runs to obtain the same amount of data.

The test results from an F5D-1 airplane modified with an ogee wing, a prototype F5D-1 airplane, two XB-70 airplanes, and an F-104A airplane indicate that theory and wind-tunnel results adequately predict the trends caused by ground effect as a function of height and aspect ratio. However, the magnitude of these predictions did not always agree with the flight-measured results. In addition, there was consistent evidence that the aircraft encountered ground effect at a height above one wing span.

17. Key Words (Suggested by Author(s)) Ground effect	18. Distribution Statement Unclassified - Unlimited		
19. Security Classif. (of this report) Unclassified	20. Security Classif. (of this page) Unclassified	21. No. of Pages 46	22. Price* $3.00

*For sale by the Clearinghouse for Federal Scientific and Technical Information
Springfield, Virginia 22151

FLIGHT EVALUATION OF GROUND EFFECT ON SEVERAL LOW-ASPECT-RATIO AIRPLANES

By Paul A. Baker, William G. Schweikhard, and William R. Young
Flight Research Center

INTRODUCTION

When an airplane flies close to the ground, at a height of one or two wing spans, it experiences an increase in lift and significant changes in drag and pitching moment. This phenomenon is known as ground effect. Interest in ground effect has recently been renewed because of its significance for both V/STOL and conventional low-aspect-ratio aircraft such as the supersonic transport. In wind-tunnel tests the effect of the ground can be simulated by moving the aircraft model progressively closer to the wind-tunnel floor or ground board. In the limited flight measurements of ground effect made in the study of reference 1, a flyby technique was used which required that an airplane be flown at a constant altitude and airspeed. Both flight and wind-tunnel methods require numerous passes or runs to obtain data throughout the altitude and angle-of-attack range.

A different flight-test method for analyzing ground effect was proposed in reference 2. With this method, a low approach is made in a test airplane while constant angle of attack and power setting are maintained. The measurement of engine thrust, which is difficult but necessary for most methods, is not required for this method because the power setting remains fixed throughout the approach. This method was used in a flight investigation at the NASA Flight Research Center in which ground effect was evaluated on five low-aspect-ratio aircraft: an F5D-1 modified with an ogee wing (ref. 3), a conventional F5D-1, two XB-70's (XB-70-1, XB-70-2), and an F-104A. These airplanes were selected because of their low aspect ratios and their similarity to some supersonic-transport configurations and because the effect of the ground on the modified F5D-1 had been measured previously using the constant-altitude-flyby technique (ref. 1).

The results of this flight study with the five airplanes are presented in this report. The measured changes in lift and pitching moment are presented as a function of the height of the airplane above the ground. The results obtained from the modified F5D-1 with the flyby method and results obtained using the constant-angle-of-attack method are compared. In addition, the data for all five airplanes are compared with wind-tunnel studies and theoretical prediction data calculated from equations presented in reference 4. At the time the constant-angle-of-attack technique was validated, the mathematical analysis associated with the theory was expanded. The expanded analysis is included in appendix A.

SYMBOLS

All quantities in this report are presented in both U. S. Customary Units and the International System of Units (SI).

b	wing span, ft (m)
C_D	drag coefficient, $\frac{\text{Drag}}{qS}$
ΔC_D	drag-coefficient increment, $C_D - C_{D_o}$
C_L	lift coefficient, $\frac{\text{Lift}}{qS}$
ΔC_L	lift-coefficient increment, $C_L - C_{L_o}$
$C_{L_{\delta_e}}$	change in lift coefficient with change in longitudinal control deflection, per deg
C_m	pitching-moment coefficient
$C_{m_{\delta_e}}$	change in pitching-moment coefficient with change in longitudinal-control deflection, per deg
$\bar{c}$	wing mean aerodynamic chord, ft (m)
D	drag force, lb (N)
ΔD	drag increment, $D - D_o$, lb (N)
g	acceleration due to gravity, ft/sec^2 (m/sec^2)
h	height of quarter chord of wing mean aerodynamic chord above ground, ft (m)
$\dot{h}$	vertical velocity, ft/sec (m/sec)
$\ddot{h}$	vertical acceleration, ft/sec^2 (m/sec^2)
h_R	height of gear above the ground, ft (m)
L	lift force, lb (N)
ΔL	lift increment, $L - L_o$, lb (N)
q	dynamic pressure, lb/ft^2 (N/m^2)
Δq	dynamic-pressure increment, $q - q_o$, lb/ft^2 (N/m^2)

S	wing area, ft^2 (m^2)
T	aircraft net thrust, lb (N)
t	time, sec
V	true velocity, ft/sec (m/sec)
W	aircraft weight, lb (kg)
x	horizontal distance, ft (m)
$\dot{x}$	horizontal velocity, ft/sec (m/sec)
$\ddot{x}$	horizontal acceleration, ft/sec^2 (m/sec^2)
α	angle of attack, deg
γ	flight-path angle, deg
δ_e	longitudinal-control-surface deflection, deg
$\Delta\delta_e$	longitudinal-control-surface-deflection increment, $\delta_e - \delta_{e_o}$, deg
θ	pitch-attitude angle, deg

Subscript:

o	initial value

TEST AIRCRAFT

The airplanes used in the program were a Douglas prototype F5D-1 modified with an ogee wing, a conventional Douglas prototype F5D-1, the two North American XB-70's, and a Lockheed F-104A. The pertinent dimensions for each airplane are given in table 1, and three-view drawings of the airplanes are shown in figures 1 to 4. The modified F5D-1 airplane has a planform similar to that of the Concorde (ref. 5). It has an aspect ratio of 1.70, whereas the conventional F5D-1 airplane has an aspect ratio of 2.0. Each of the XB-70 airplanes has an aspect ratio of 1.75, with a size and weight similar to the foreign and domestic supersonic transports (refs. 5 and 6). The F5D-1 and XB-70 airplanes have delta wings and elevons for their main control surfaces. The F-104A airplane, with an aspect ratio of 2.45, has a straight wing and a high horizontal stabilizer (T-tail) which is used as an elevator.

TEST PROCEDURE AND PILOT TECHNIQUE

The technique proposed in reference 2 requires the pilot to fly the test aircraft at

a constant angle of attack and power setting during a shallow, descending approach to the runway. It was found that pilot proficiency was very important in flying approaches if useful data were to be obtained. Also, atmospheric conditions greatly affected the test results. Consequently, flights were scheduled in the early morning to take advantage of calm wind conditions and the absence of turbulence due to differential surface heating. For the two F5D-1 airplanes and the F-104A airplane, a maximum of 5 knots of surface wind was tolerated; however, for the larger and heavier XB-70 airplanes, usable data were obtained with winds as high as 11 knots.

The Air Force Flight Test Center (AFFTC) tracking facility provides optimum data when an airplane is near the midpoint on the runway. It was found that a glide-slope indicator light (fig. 5) aided the pilot in establishing the initial conditions of constant angle of attack and steady sink rate. The indicator was used as a reference from which to initiate the airplane's descent so that it would be in the proximity of the ground near the midpoint of the runway.

In the F5D-1 airplanes and the F-104A airplane, the angle-of-attack display was placed just inside the windshield directly in front of the pilot. This location enabled the pilot to determine his relationship to the ground without interrupting his concentration on angle of attack. Because of lack of space in the windshield area, the normal location for the angle-of-attack display was used in the XB-70 airplanes.

DATA ACQUISITION AND ANALYSIS

Aircraft Instrumentation

Each of the airplanes was instrumented to record angle of attack and control-surface deflection. In addition, the XB-70 aircraft were instrumented to record power-lever position. The accuracies and ranges of the sensors installed in each airplane are listed in table 2. Also listed are the ranges and resolutions of the cockpit angle-of-attack displays. Time correlation was attained by using a tone switch mounted on each of the pilot's control sticks or columns. When on, the switch transmitted a 1000-cycle-per-second tone over the UHF communication channel which was received by the tracking facility.

Tracking Facility

The AFFTC Takeoff and Landing Facility provided the external tracking required for the program. The Facility maintains two Askania cinetheodolite stations, one near each end of the main runway, as shown in figure 6. Precision position data as a function of time were obtained from the Facility during each low approach. Wind speed, wind direction, and air temperature were also recorded by the Facility. The installation is described in detail in reference 7.

Method of Analysis

In addition to the assumptions of constant angle of attack and power setting, the constant-angle-of-attack technique assumes a shallow flight path ($\gamma \leqq 3°$). While

approaching the runway, the pilot establishes the initial conditions. The angle of attack corresponds to a particular speed and the power setting to a particular sink rate. These steady-state conditions are disturbed by ground effect, causing the aircraft to change both speed and sink rate. The relationship between these accelerations and the normalized lift coefficient is given by the following equation:

$$\frac{\Delta C_L}{C_{L_o}} = \frac{q_o}{q}\left[\left(\frac{\ddot{h}}{g}\cos\gamma - \frac{\ddot{x}}{g}\sin\gamma + \cos\gamma\right) - \left(\frac{\ddot{h}_o}{g}\cos\gamma_o - \frac{\ddot{x}_o}{g}\sin\gamma_o + \cos\gamma_o\right)\right] - \frac{\Delta q}{q} \quad (1)$$

Data Reduction

The Askania cinetheodolite camera system began tracking the test airplane's descent when it was approximately 200 feet (61 meters) above the ground. Because the airplane was still out of ground effect, initial sink rates and approach speeds could be determined. The parameters provided by the tracking facility and atmospheric pressures obtained from the Edwards Air Force Base weather station were used as inputs to a computer program which calculated the aircraft's vertical and horizontal position and dynamic pressure each one-fourth second during a run.

The time history in figure 7 of an approach made in an XB-70 airplane is typical of the data that can be obtained with the constant-angle-of-attack-approach technique. As required, the throttle angle was absolutely constant. The angle of attack decreased slightly, but the increase in lift due to ground proximity still caused the airplane to flare. Corrections were applied for minor deviations from the reference angle of attack. Ground effect also changed the pitching moment. The 3° to 4° change in elevon deflection was required to maintain angle of attack. The eventual decrease of 10 ft/sec (3.1 m/sec) in true velocity is qualitative evidence of increased drag resulting from the nearness of the ground; however, conclusive quantitative analysis of these data in terms of drag increments was not possible.

The position data calculated by the computer were reduced to obtain the vertical and horizontal velocities and accelerations. Two methods were used to obtain $\dot{h}$, $\dot{x}$, $\ddot{h}$, and $\ddot{x}$. One method was to plot the altitude versus time and then fit a smooth curve to the points. The slopes of the resulting curve represented the rate of sink at each time interval. Similarly, plotting the horizontal position versus time and taking slopes provided horizontal velocity. Repeating the procedure by plotting rate of sink and horizontal velocity versus time produced the required vertical and horizontal accelerations.

The quantities $\ddot{h}$ and $\ddot{x}$ were also obtained from the following relationships:

$$\ddot{h} = \frac{dh}{dt}\frac{1}{\frac{dh}{d\left(\frac{dh}{dt}\right)}} \quad (2)$$

$$\ddot{x} = \frac{dh}{dt}\frac{1}{\frac{dh}{d\left(\frac{dx}{dt}\right)}} \quad (3)$$

The rate of sink and horizontal velocity were obtained in the manner described in the preceding paragraph. The slopes from a curve of altitude versus rate of sink represent the quantity $\frac{dh}{d\left(\frac{dh}{dt}\right)}$. Similarly, the slopes of the curve of altitude versus horizontal velocity represent $\frac{dh}{d\left(\frac{dx}{dt}\right)}$. Once the accelerations were obtained, they were used in equation (1) to calculate the normalized increase in lift coefficient.

Obtaining the vertical and horizontal accelerations by either of these methods was tedious. Consequently, several computer smoothing routines were tried to determine if they could fit the plotted curves, but none was able to do a satisfactory job. They were overly influenced by stray points and calculated extraneous accelerations.

PRECISION

Accuracy of the Position Measurement

The accuracy of the position data from the tracking facility was evaluated (ref. 7) to be ±1.5 feet (±0.5 meter). Further, the velocities and accelerations obtained from the hand reduction methods are accurate within ±0.3 ft/sec (±0.1 m/sec) and ±0.06 ft/sec^2 (±0.02 m/sec^2), respectively. From these values, the variation in dynamic pressure was calculated to be ±0.5 lb/ft^2 (±2.4 N/m^2).

Accuracy of the Angle-of-Attack Measurement

Because the low approaches were flown at constant angles of attack, only the changes in the influence of upwash in and out of ground effect on the angle-of-attack vane affected the data. A comparison of onboard and Askania measurements indicated no perceptible change in upwash influence on the vane.

Because lift varies sharply with angle of attack, deviations in this angle during an approach caused significant changes in the measured results. Hence, any deviations which occurred were corrected by using wind-tunnel data from the sources listed in table 3.

RESULTS AND DISCUSSION

The results of the ground-effect tests are shown as a function of quarter-chord height and angle of attack in figures 8 to 20. The lift increments are presented as percent increases in the lift coefficient, and the pitching-moment change is indicated by the deviation of the longitudinal-control input from the out-of-ground-effect trim condition. The basic aerodynamic characteristics for each aircraft, obtained from references 8 and 9 and unpublished data, are presented in appendix B. Because

longitudinal-control inputs also cause changes in lift, the trim change is responsible for the difference between the percent increase in the trimmed and untrimmed lift-coefficient increments shown. The untrimmed lift coefficient represents the lift which could be expected if there were no trim change. Moreover, it allows direct comparison with wind-tunnel and theoretical results.

It should be pointed out that each set of symbols representing the data for one angle of attack was obtained from one approach. The initial and final values of the control-surface position, airspeed V, sink rate $\dot{h}$, dynamic pressure q, and flight-path angle γ for each of the data runs are tabulated in tables 4 to 7.

General Comments and Observations

In every approach the aircraft encountered increased trimmed and untrimmed lift increments and an increased negative pitching moment as they approached the ground. With the exception of the XB-70, measurable lift increments were experienced above the classic one wing span; however, significant effects were not encountered until the airplane descended to lower heights. These lift increments generally preceded any measurable pitching-moment changes.

The pilots in the program made several qualitative observations about the extent of ground effect encountered. There were consistent comments on the strong flare and float characteristics of the F-104A airplane, whereas the XB-70 airplanes were noted to become more stable laterally. On the other hand, the F5D-1 airplanes did not "float" as much as the XB-70 and F-104A airplanes. Quantitatively, the flare and float characteristics can be related to the airplane's initial sink rate. An initial sink rate as low as 4.3 ft/sec (1.3 m/sec) caused the F5D-1 airplanes to touch down; whereas, on one approach the XB-70 airplanes had an initial sink rate of 7.3 ft/sec (2.2 m/sec) but did not touch down. Similarly, the increase in the lift of the F-104 airplane due to ground effect reduced sink rates of 20 ft/sec (6.1 m/sec) to zero and caused the airplane to stabilize a few feet above the runway for the rest of the approach.

A mathematical analysis of the drag change due to ground effect is presented in appendix A; however, attempts to quantitatively measure the change in drag produced inconsistent results. The problem is believed to lie with the relatively small magnitudes of the accelerations that must be measured. These accelerations are easily lost among the inadvertent inputs associated with flying the airplane. Although the change in drag was not measured, some deductions were made by observing the change in true airspeed during the low approaches. As an approximation, a reduction in true airspeed may be interpreted as an increase in drag, and an increase in true airspeed, as a reduction in drag. On the basis of the general reduction in speed (tables 4 to 7), it appears that the drag generally increased as the airplane encountered ground effect during the constant-angle-of-attack approaches. Analytical methods and test techniques for extracting drag data due to ground effect need further research.

F5D-1 Airplane Modified With an Ogee Wing

The effect of ground proximity on the lift and pitching moment of the modified F5D-1 airplane is shown in figure 8. As can be seen, the pitching moment due to

ground effect is small (less than 1° change in elevon position). Consequently, the trimmed and untrimmed lift increments are approximately equal at 24 percent at touchdown.

A comparison of flight results obtained by two different flight-test techniques is shown in figure 9. In the constant-altitude-flyby tests of reference 1, measurements were assigned altitude bands rather than discrete heights; consequently, in this figure, the horizontal line is at the center of the original altitude band, and its length covers the spread of the data within that band. The vertical line at each end of the horizontal line symbolizes the width of the band. The individual measurements within each band are indicated by the tick marks on the horizontal line. These data are superimposed on the constant-angle-of-attack-approach data from figure 8. Although the lift-coefficient data show general agreement at the lower heights, the constant-angle-of-attack data are more consistent than the constant-altitude-flyby data. The disparity between the two sets of data increases with increasing airplane height above the ground. Also, it should be noted that the constant-angle-of-attack data were obtained during 5 runs, whereas the constant-altitude-flyby data required 44 runs.

Figure 10 is a comparison of wind-tunnel data and theoretical predictions with data from a 10° constant-angle-of-attack approach. As can be seen, the flight data and the predicted data from reference 4 are in close agreement in both trend and magnitude; however, extrapolating the wind-tunnel results indicates a lift increment near the ground substantially greater than either the flight or reference 4 results. On the other hand, it should be noted that the wind-tunnel data go to zero below one wing span, but the flight and analytical results show lift increments above one wing span. It seems reasonable that the wind-tunnel incremental-lift results go to zero at lower heights because of the negative effect produced by the ceiling of the tunnel. This is especially true of the full-scale tests in which the model is nearly in the center of the tunnel at the one-half span, and, as expected, the ground effect measured in the tunnel is zero.

Flight, wind-tunnel, and theoretical ground-effect data for the modified F5D-1 are summarized in figure 11 as a function of angle of attack at 0.30 wing span. There is some correlation of trends but little correlation of magnitudes between the various sources of data. The NASA Ames Research Center's constant-altitude-flyby and wind-tunnel data and the data of reference 4 indicate a slightly decreasing incremental lift coefficient with increasing angle of attack. On the other hand, the constant-angle-of-attack flight data and the NASA Langley Research Center and Lockheed wind-tunnel data indicate increasing incremental lift coefficient with increasing angle of attack. All the wind-tunnel pitching-moment data show the same increasing trend with angle of attack; however, both sets of flight results indicate a relatively constant trim change with angle of attack.

Basic F5D-1 Airplane

Figure 12 shows the effect of ground proximity on the lift coefficient and elevon deflection for the basic F5D-1 airplane. The results are similar to those for the modified F5D-1 airplane, in that there is little change in pitching moment due to entering ground effect, as indicated by the small change in elevon position (0° to 2.4°). Consequently, the trimmed and untrimmed increases in lift coefficient are nearly the same, increasing to approximately 14 percent at touchdown. The difference between

this lift increment and the 24-percent value for touchdown of the modified F5D-1 airplane (fig. 8) shows the influence of the planform modifications.

In figure 13, a typical midrange angle-of-attack approach for the basic F5D-1 airplane is compared with corresponding reference 4 data and wind-tunnel results. The increase in lift coefficient predicted by reference 4 agrees well with the flight results; however, the wind-tunnel measurement is considerably higher than either the prediction or the flight data. The trim changes shown by the reference 4 and wind-tunnel results were both substantially greater than the flight-measured change.

In figure 14 the flight, wind-tunnel, and reference 4 results indicate similar trends in change in lift coefficient with angle of attack but differ with regard to the magnitude of the change. Both the wind-tunnel and reference 4 data predict greater lift increments in ground effect than were measured in flight. Similarly, the reference 4 and wind-tunnel data suggest a greater trim change than was measured in flight. The flight-measured trim changes also indicate no functional dependence on angle of attack, whereas the predicted and wind-tunnel data indicate an increasing trim change with increasing angle of attack.

XB-70 Airplanes

The effect of the ground on the lift and pitching moment of the XB-70 airplanes is shown in figure 15. Because the only difference between the two aircraft is a positive 5° dihedral of the wing on the XB-70-2 airplane, the results from approaches made by both aircraft are plotted in the same figure. Again the results show that the trim change and incremental lift coefficient increase as the airplane approaches the ground. At touchdown the trimmed and untrimmed lift coefficients increase to approximately 18 percent and 24 percent, respectively. The elevon increment of the XB-70 is large compared with that for the F5D-1 airplane, probably because the XB-70 elevons are less effective than those of the F5D-1 airplane. Significant changes begin below one wing span and increase to 3° or 4° change in elevon deflection at touchdown.

It may be noted that these results do not necessarily agree with the XB-70 results in references 3 and 10. The data from these references are from early flights that were not specifically flown to obtain ground-effect data. It appeared that the data used in those references met all the criteria for the descent method described herein except for seemingly small variations of approximately 1° in angle of attack and 500 pounds (2224 newtons) to 1000 pounds (4448 newtons) in thrust. It was thought that corrections could be made for these variations; however, subsequent experience showed that the magnitudes of the corrections were greater than the ground effect being measured. Consequently, the adequacy of the correction became very sensitive to inaccuracies in the wind-tunnel data upon which the corrections were based. The most useful data are obtained when the magnitude of the correction is kept to a minimum.

The greater scatter in the XB-70 untrimmed lift data as compared with the F5D-1 data is probably due to a stronger dependence of the XB-70 lift increment on angle of attack, as indicated in figure 16. Both the wind-tunnel and the reference 4 predictions follow the same trends in the changes in lift with angle of attack. The flight data diverge from these trends at the higher angles of attack, but they are generally interspersed with the other data. The change in elevon deflection with angle of attack

agrees well with the NASA Langley Research Center wind-tunnel results above an angle of attack of 8°. In addition, the trends are similar for both wind-tunnel and reference 4 predictions at these higher angles.

Figure 17 compares flight, wind-tunnel, and predicted ground-effect data for the XB-70 airplanes for an angle of attack of 9.3°. The 7- by 10-foot wind-tunnel data are unpublished results obtained from tests on a 0.03-scale model at the NASA Langley Research Center. Although the general trend for the increase in lift and the trim change is the same for all three sets of data, there is considerable disparity in the magnitudes of the results. The lift increment predicted by reference 4 is lower than that shown by the flight data, but the pitching moment is higher. At touchdown, however, the flight data lift and pitching-moment results lie between the results of the two wind-tunnel measurements. As shown previously for the modified F5D-1 airplane, the wind-tunnel ground-effect data go to zero prematurely; whereas, the flight and reference 4 results indicate ground effect up through one wing span.

F-104A Airplane

As shown in figure 18, the influence of the ground on the F-104A airplane was found to begin at a height well above one wing span but did not reach a significant magnitude until the airplane was below a height of 0.6 wing span. Below 0.6 wing span, the effect increases quite rapidly to a maximum near touchdown, where both the trimmed and untrimmed lift coefficients indicate increases near 20 percent. Sufficient flight data were not available near touchdown for a meaningful comparison because the pilots found it difficult to touch down while holding constant angle of attack. Touchdown was experienced only when the initial rates of descent were very high, greater than 24.0 ft/sec (7.3 m/sec). Similar to the F5D-1 airplanes, the trim change measured on the F-104A airplane was less than 1° of stabilizer. This is attributed to the fact that the high horizontal stabilizer on the F-104A airplane is outside the flow field of the wing and is never close enough to the ground to experience ground effect.

Figure 19 compares flight, wind-tunnel, and predicted ground-effect data for an angle of attack of 6.9°. Although the incremental lift predicted from reference 4 data is slightly low when compared with the flight results, the wind-tunnel and predicted pitching moments agree well with the flight data.

Figure 20 shows the variation of lift and pitching moment with angle of attack at touchdown heights for which wind-tunnel data were available. Only slight reductions in lift increment with increasing angle of attack are indicated by the predicted and the wind-tunnel results, whereas the flight results indicate an increasing trend. A possible reason for the low lift increment predicted by reference 4 could be the negative dihedral angle of the F-104A airplane which places the wing tips closer to the ground than the projection of the quarter chord on the wing root that was used as the basis of the prediction. The pitching-moment changes with angle of attack shown by the flight and the wind-tunnel results agree, but the predicted data do not.

Although this observation is not readily rationalized on the basis of the data presented in figure 18, wind-tunnel data (see appendix B) indicate that the lift increase is greater than 25 percent of the free-air value. Flight data were difficult to obtain in this region because the pilot felt that the nosewheel would contact the ground first at these high sink rates.

Summary of Results

Trends predicted by using the data of reference 4 agree with flight results; however, the magnitudes of the data do not. The predicted lift increments are lower than those measured in flight for all the low-aspect-ratio configurations tested. Similarly, at the higher heights wind-tunnel measurements underpredicted the lift increment due to ground effect, possibly due to the effects of the tunnel ceiling as the model approached the centerline of the tunnel. Pitching-moment changes due to ground effect predicted by reference 4 were consistently high at all heights for all delta-wing configurations tested; however, the F-104 flight results were predicted correctly. One important point concerning predictions of lift increment due to ground effect is that the trim change always results in reduction of the trimmed lift increments that will be experienced in flight such that in extreme instances in which the untrimmed lift increment is small and the pitching-moment change is large it is possible to experience negative trimmed lift increments in flight.

Because the aircraft tested represent a cross section of planform, an attempt was made to correlate the flight results at 0.20, 0.30, and 0.40 wing span with the results predicted by reference 4 at corresponding conditions. Figure 21 compares flight data with the prediction for a conventional airplane with a horizontal stabilizer and a delta-wing airplane. The figure shows the increased lift increment that should be expected for the lower-aspect-ratio planforms. The lift increments shown by the flight data are consistently higher than predicted at all heights for all the aircraft tested. Although the flight results tend to follow the same trends, more data on higher-aspect-ratio aircraft are needed before aspect-ratio effects can be established conclusively.

CONCLUDING REMARKS

A constant-angle-of-attack-approach technique was used to obtain ground-effect data on several low-aspect-ratio aircraft. These flight results were compared with results obtained from constant-altitude-flybys, wind-tunnel studies, and theoretical prediction data. The test results indicated that the constant-angle-of-attack technique provided data consistent with those obtained from the constant-altitude-flyby method and required fewer runs to obtain the same amount of data.

As was expected, when the test aircraft approached the ground, ground effect caused significant changes in lift, drag, and pitching moment. Although the trends of these changes agreed with the theoretical and wind-tunnel predictions, the magnitudes did not. The measured lift increments were consistently higher than the theoretical prediction, whereas the measured pitching moment was generally less. Improved prediction methods are required to determine the magnitudes of the lift and pitching-moment changes. The consistent evidence of ground effect above one wing span and the qualitative pilot comments on the improvement in handling qualities of the XB-70 and F-104A airplanes while in ground effect were unexpected.

APPENDIX A

DERIVATION OF GROUND-EFFECT EQUATION

The forces acting on an airplane during a shallow, constant-angle-of-attack approach are shown in the following sketch:

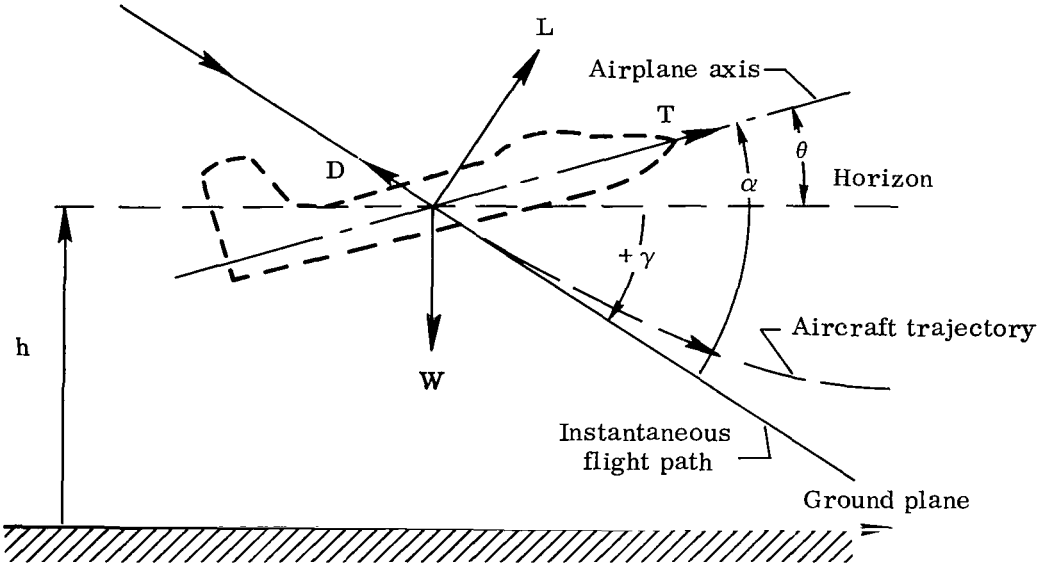

First, summing the forces perpendicular to the flight path,

$$L + T \sin \alpha - W \cos \gamma = \frac{W}{g}(\ddot{h} \cos \gamma + \ddot{x} \sin \gamma)$$

Solving for the lift,

$$L = \frac{W}{g}(\ddot{h} \cos \gamma + \ddot{x} \sin \gamma) + W \cos \gamma - T \sin \alpha$$

The initial lift is given by

$$L_o = \frac{W_o}{g}(\ddot{h}_o \cos \gamma_o + \ddot{x}_o \sin \gamma_o) + W_o \cos \gamma_o - T_o \sin \alpha$$

As indicated in reference 2, the constant-angle-of-attack-approach technique requires that angle of attack and throttle be held constant. This results in thrust remaining constant throughout the approach because there is no change in the inlet recovery as long as angle of attack is constant. Also, the change in thrust due to a change in density is very small because the altitude range is small. Weight may also be assumed to be constant ($W \approx W_o$), since the run is of short duration (less than

30 seconds) and the power setting is low. Therefore, thrust, weight, and angle of attack are treated as constants in this analysis. Thus, the equation

$$\frac{\Delta L}{W} = \frac{L - L_o}{W}$$

becomes

$$\frac{\Delta L}{W} = \left(\frac{\ddot{h}}{g}\cos\gamma + \frac{\ddot{x}}{g}\sin\gamma + \cos\gamma\right) - \left(\frac{\ddot{h}_o}{g}\cos\gamma_o + \frac{\ddot{x}_o}{g}\sin\gamma_o + \cos\gamma_o\right) \qquad \text{(A1)}$$

For $\gamma \leqq 3°$

$$L_o \approx L_o \cos\gamma_o = W_o \approx W$$

or

$$L_o \approx W$$

and

$$\frac{\Delta L}{L_o} = \left(\frac{\ddot{h}}{g}\cos\gamma + \frac{\ddot{x}}{g}\sin\gamma + \cos\gamma\right) - \left(\frac{\ddot{h}_o}{g}\cos\gamma_o + \frac{\ddot{x}_o}{g}\sin\gamma_o + \cos\gamma_o\right) \qquad \text{(A2)}$$

It is also true that

$$\Delta L = L - L_o = C_L qS - C_{L_o} q_o S$$

Dividing by $L_o = C_{L_o} q_o S$,

$$\frac{\Delta L}{L_o} = \frac{C_L qS}{C_{L_o} q_o S} - 1$$

then canceling S and substituting $C_L = \Delta C_L + C_{L_o}$,

$$\frac{\Delta L}{L_o} = \frac{\Delta C_L q}{C_{L_o} q_o} + \frac{q}{q_o} - 1$$

Since $q = \Delta q + q_o$,

$$\frac{\Delta L}{L_o} - \frac{\Delta C_L q}{C_{L_o} q_o} = \frac{\Delta q}{q_o}$$

or

$$\frac{\Delta C_L}{C_{L_o}} = \frac{\Delta L q_o}{L_o q} - \frac{\Delta q}{q} \tag{A3}$$

Substituting from equation (A2) yields the following expression (eq. (1)):

$$\frac{\Delta C_L}{C_{L_o}} = \frac{q_o}{q}\left[\left(\frac{\ddot{h}}{g}\cos\gamma + \frac{\ddot{x}}{g}\sin\gamma + \cos\gamma\right) - \left(\frac{\ddot{h}_o}{g}\cos\gamma_o + \frac{\ddot{x}_o}{g}\sin\gamma_o + \cos\gamma_o\right)\right] - \frac{\Delta q}{q}$$

This, then, is the final equation for analyzing the lift increment due to ground effect.

Now, summing the forces tangential to the flight path,

$$T\cos\alpha - D + W\sin\gamma = \frac{W}{g}(\ddot{x}\cos\gamma - \ddot{h}\sin\gamma)$$

Solving for D and following the same procedure as was used to obtain equation (A2),

$$\frac{\Delta D}{L_o} = \left(\frac{\ddot{x}_o}{g}\cos\gamma_o - \frac{\ddot{h}_o}{g}\sin\gamma_o - \sin\gamma_o\right) - \left(\frac{\ddot{x}}{g}\cos\gamma - \frac{h}{g}\sin\gamma + \sin\gamma\right) \tag{A4}$$

Likewise,

$$\Delta D = D - D_o = C_D q S - C_{D_o} q_o S$$

and

$$q = q_o + \Delta q$$

so

$$\Delta D = \left(C_D - C_{D_o}\right) q_o S + C_D \Delta q S$$

Then, normalizing with respect to the initial lift,

$$\frac{\Delta D}{L_o} = \frac{\left(C_D - C_{D_o}\right) q_o S}{C_{L_o} q_o S} + \frac{\Delta q \left(C_D - C_{D_o}\right) S}{C_{L_o} q_o S} + \frac{C_{D_o} \Delta q S}{C_{L_o} q_o S}$$

because

$$\Delta C_D = C_D - C_{D_o}$$

and

$$\frac{\Delta D}{L_o} = \frac{\Delta C_D}{C_{L_o}} \frac{(q_o + \Delta q)}{q_o} + \frac{C_{D_o} \Delta q}{C_{L_o} q_o} = \frac{\Delta C_D q}{C_{L_o} q_o} + \frac{C_{D_o} \Delta q}{C_{L_o} q_o}$$

which, upon rearrangement, gives

$$\frac{\Delta C_D}{C_{L_o}} = \left(\frac{\Delta D}{L_o} - \frac{C_{D_o} \Delta q}{C_{L_o} q_o} \right) \frac{q_o}{q}$$

Substituting from equation (A4),

$$\frac{\Delta C_D}{C_{L_o}} = \frac{q_o}{q} \left[\left(\frac{\ddot{x}_o}{g} \cos \gamma_o - \frac{\ddot{h}_o}{g} \sin \gamma_o - \sin \gamma_o \right) - \left(\frac{\ddot{x}}{g} \cos \gamma - \frac{\ddot{h}}{g} \sin \gamma - \sin \gamma \right) \right] - \frac{C_{D_o} \Delta q}{C_{L_o} q} \quad \text{(A5)}$$

However, $\frac{C_{D_o}}{C_{L_o}} = \frac{D}{L}$, which may be obtained from wind-tunnel data.

Therefore, equation (A5) becomes

$$\frac{\Delta C_D}{C_{L_o}} = \frac{q_o}{q} \left[\left(\frac{\ddot{x}_o}{g} \cos \gamma_o - \frac{\ddot{h}_o}{g} \sin \gamma_o - \sin \gamma_o \right) - \left(\frac{\ddot{x}}{g} \cos \gamma - \frac{\ddot{h}}{g} \sin \gamma - \sin \gamma \right) \right] - \frac{D}{L} \frac{\Delta q}{q} \quad \text{(A6)}$$

which is the final equation for the analysis of the drag increment due to ground effect.

APPENDIX B

WIND-TUNNEL DATA

Throughout this report, comparisons have been made between the flight results and wind-tunnel results obtained from both published and unpublished sources. The wind-tunnel comparison data are presented in more complete form in figures 22 to 25. Figure 22 presents data from reference 1 on the F5D-1 airplane modified with an ogee wing. Wind-tunnel data from reference 8 for the basic F5D-1 airplane are presented in figure 23. In figure 24 unpublished data obtained in the Langley 7- by 10-foot wind tunnel with a moving-belt ground plane are shown for the XB-70 airplane. Lockheed wind-tunnel data on the F-104A airplane were obtained from several unpublished reports and are shown in figure 25.

REFERENCES

1. Rolls, L. Stewart; and Koenig, David G.: Flight-Measured Ground Effect on a Low-Aspect-Ratio Ogee Wing Including a Comparison With Wind-Tunnel Results. NASA TN D-3431, 1966.

2. Schweikhard, William: A Method for In-Flight Measurement of Ground Effect on Fixed-Wing Aircraft. J. Aircraft, vol. 4, no. 2, March-April 1967, pp. 101-104.

3. Rolls, L. Stewart; Koenig, David G.; and Drinkwater, Fred J. III: Flight Investigation of the Aerodynamic Properties of an Ogee Wing. NASA TN D-3071, 1965.

4. Anon.: USAF Stability and Control Datcom. Air Force Flight Dynamics Lab., Wright-Patterson Air Force Base, Oct. 1960 (rev. Aug. 1968).

5. Anon.: Specifications. Aviation Week & Space Technology, March 18, 1968, pp. 192, 204.

6. Winston, Donald C.: Aeroflot Accelerates Plans to Place SST into Commercial Service. Aviation Week & Space Technology, July 29, 1968, pp. 24, 25.

7. Taylor, Albert E.: Evaluation of Take-off and Landing Facility. Tech. Memo. FTFF-TM-58-12, U.S. Air Force Flight Test Center, Apr. 1958.

8. Radoll, R. W.: Aerodynamic Data for Model F5D-1 Operational Flight Trainer. Rep. No. ES 26257 (Contract No. NOa(s) 54-321), Douglas Aircraft Co., Inc., Apr. 26, 1956.

9. Bowman, Paul V.: Estimated Performance Report for the XB-70A Air Vehicle No. 2. NA-65-661, North American Aviation, Inc., July 26, 1965.

10. Rolls, L. Stewart; Snyder, C. Thomas; and Schweikhard, William G.: Flight Studies of Ground Effects on Airplanes With Low-Aspect-Ratio Wings. Conference on Aircraft Aerodynamics, NASA SP-124, 1966, pp. 285-295.

TABLE 1. – DIMENSIONAL AND AERODYNAMIC DATA FOR THE TEST AIRPLANES

	Modified F5D-1	Basic F5D-1	XB-70	F-104A
S, ft^2 (m^2)	661.0 (61.4)	557.0 (51.8)	6296.0 (585.0)	196.1 (18.2)
b, ft (m)	33.5 (10.2)	33.5 (10.2)	105 (32)	21.9 (6.7)
$\bar{c}$, ft (m)	22.6 (6.9)	18.3 (5.6)	78.5 (23.9)	9.6 (2.9)
Leading-edge sweep, deg	77.0	52.5	51.8	18.1
Dihedral, deg	0	0	0, XB-70-1 5, XB-70-2	-10
Fuselage length, ft (m)	46.8 (14.3)	46.8 (14.3)	185.75 (56.62)	52.4 (16.0)
h at touchdown, ft (m)	6.1 (1.9)	5.0 (1.5)	17 (5.2)	4.6 (1.4)
Aspect ratio	1.70	2.0	1.75	2.45
Elevon area, ft^2 (m^2)	24.3 (2.3)	26.0 (2.4)	197.7 (18.4)	48.2 (4.5)
Dry weight, lb (kg)	19,000 (8,620)	17,800 (8,080)	264,000 (120,000)	13,700 (6,220)
$C_{L_{\delta_e}}$	0.0155	0.0162	0.00945	0.01025 at $\delta_e = 4°$ 0.013 at $\delta_e = 8°$
$C_{m_{\delta_e}}$	-0.0063	-0.006 at $\alpha = 4°$ -0.0054 at $\alpha = 12°$ -0.0051 at $\alpha = 16°$	-0.0365 at h/b > 0.3 -0.0340 at h/b = 0.2 -0.0310 at h/b = 0.15	-0.0270

TABLE 2. – ACCURACIES OF AIRCRAFT SENSORS AND RANGE AND RESOLUTION OF COCKPIT DISPLAYS

		Modified F5D-1	Basic F5D-1	XB-70	F-104A
α, deg	Sensor accuracy Indicator range Indicator resolution	0.4 5 to 19 0.25	0.4 5 to 19 0.25	0.3 -10 to 30 0.50	0.4 5 to 19 0.25
δ_e, deg	Instrument accuracy Instrument range (trailing edge up, positive)	0.50 18 to -20	0.50 18 to -20	0.72 30 to -30	0.50 6 to -17
Power-lever position, deg	Instrument accuracy Instrument range	-------- --------	-------- --------	1.5 0 to 125	------- -------

TABLE 3. – SOURCES OF WIND-TUNNEL DATA FOR THE AIRPLANES TESTED

Airplane	Source	Facility	Scale of model	Ground plane
Modified F5D-1	Reference 1	Ames 40- by 80-foot wind tunnel	Full scale	Fixed
		Lockheed 8- by 12-foot tunnel	0.15	Fixed
		Langley 7- by 10-foot wind tunnel	.15	Moving belt
Basic F5D-1	Reference 8	California Institute of Technology 10-foot low speed wind tunnel (GALCIT)	0.15	Fixed
XB-70	Reference 9	North American 7.75- by 11-foot low-speed wind tunnel	0.03	Fixed
		Langley 7- by 10-foot wind tunnel	.03	Moving belt
F-104	Manufacturer	Lockheed Aerodynamics Laboratory 8 × 12 foot wind tunnel	0.17	Fixed

TABLE 4. – INITIAL AND FINAL VALUES OF SIGNIFICANT PARAMETERS MEASURED ON THE APPROACHES MADE IN THE F5D-1 AIRPLANE MODIFIED WITH AN OGEE WING

Run	α, deg	Control-surface position, deg		V, ft/sec (m/sec)		$\dot{h}$, ft/sec (m/sec)		q, lb/ft^2 (N/m^2)		γ, deg	
		Initial	Final	Initial	Final	Initial	Final	Initial	Final	Initial	Final
1	9.4	3.6	4.4	293.8 (89.6)	286.1 (87.2)	6.0 (1.8)	0.8 (0.2)	93.7 (449)	88.9 (426)	1.2	0.2
2	10.0	4.0	5.1	285.8 (87.1)	274.3 (83.6)	10.8 (3.3)	-.8 (-.3)	88.6 (4240)	81.6 (3910)	2.2	0
3	11.9	1.8	2.6	249.7 (76.1)	248.4 (75.7)	13.1 (4.0)	4.3 (1.3)	76.8 (3680)	76.1 (3640)	3.0	1.0
4	13.4	4.3	4.6	254.9 (77.7)	257.8 (78.6)	7.6 (2.3)	5.3 (1.6)	77.7 (3720)	79.4 (3800)	1.7	1.2
5	14.4	4.4	5.1	246.1 (75.0)	243.8 (74.3)	13.6 (4.2)	1.2 (.4)	73.7 (3530)	72.4 (3470)	3.2	.3

TABLE 5. – INITIAL AND FINAL VALUES OF SIGNIFICANT PARAMETERS MEASURED ON THE APPROACHES MADE IN THE BASIC F5D-1 AIRPLANE

Run	α, deg	Control-surface position, deg		V, ft/sec (m/sec)		$\dot{h}$, ft/sec (m/sec)		q, lb/ft^2 (N/m^2)		γ, deg	
		Initial	Final	Initial	Final	Initial	Final	Initial	Final	Initial	Final
1	11.1	2.9	2.9	404.3 (123.2)	398.7 (121.5)	9.5 (2.9)	1.6 (0.5)	181.2 (8670)	176.8 (8470)	1.3	0.2
2	14.4	3.5	4.2	307.3 (93.7)	303.0 (92.4)	8.1 (2.5)	1.4 (.4)	104.9 (5020)	101.9 (4880)	1.7	.1
3	15.8	6.8	7.4	314.0 (95.7)	311.1 (94.8)	8.0 (2.4)	1.3 (.4)	109.8 (5260)	108.2 (5180)	1.5	.2
4	16.0	5.8	5.9	317.0 (96.6)	313.4 (95.5)	6.8 (2.1)	1.4 (.4)	111.2 (5320)	108.7 (5200)	1.2	.2
5	16.6	2.5	2.5	338.0 (103.0)	335.5 (102.3)	10.5 (3.2)	4.3 (1.3)	120.4 (5770)	118.6 (5680)	1.8	.7
6	17.2	4.7	5.5	340.2 (103.7)	328.5 (100.1)	12.7 (3.9)	1.5 (.5)	124.7 (5970)	116.2 (5560)	2.1	.3
7	17.5	5.7	8.1	269.5 (82.1)	264.1 (80.5)	5.8 (1.8)	1.1 (.3)	80.8 (3870)	77.3 (3700)	1.2	.3
8	19.0	5.6	6.2	308.7 (94.1)	299.9 (91.4)	4.7 (1.4)	3.6 (1.1)	98.9 (4730)	93.2 (4460)	.9	.7
9	19.5	4.9	4.9	330.0 (100.6)	317.8 (96.9)	14.7 (4.5)	2.1 (.6)	118.0 (5650)	110.0 (5270)	2.6	.4

TABLE 6. – INITIAL AND FINAL VALUES OF SIGNIFICANT PARAMETERS MEASURED ON THE APPROACHES MADE IN THE XB-70 AIRPLANES

Run	α, deg	Control-surface position, deg		V, ft/sec (m/sec)		$\dot{h}$, ft/sec (m/sec		q, lb/ft^2 (N/m^2)		γ, deg	
		Initial	Final	Initial	Final	Initial	Final	Initial	Final	Initial	Final
1	6.0	12.5	14.8	412.0 (125.6)	383.7 (117.0)	6.3 (1.9)	1.3 (0.4)	191.9 (9190)	167.2 (8010)	0.9	0.2
2	6.2	10.8	13.8	392.7 (119.7)	355.9 (108.5)	5.4 (1.6)	3.0 (.9)	147.8 (7080)	121.9 (5840)	.8	.5
3	7.8	10.7	12.9	404.5 (123.3)	392.6 (119.7)	7.0 (2.1)	-.8 (-.3)	188.1 (9010)	177.3 (8490)	1.0	-.2
4	7.9	11.5	14.2	393.0 (119.8)	372.0 (113.4)	12.2 (3.7)	-.1 (-.03)	156.1 (7480)	139.6 (6690)	1.8	0
5	8.0	11.0	12.4	412.8 (125.8)	414.0 (126.2)	7.3 (2.2)	.5 (.2)	200.6 (9610)	201.8 (9660)	1.0	.1
6	8.2	9.8	11.6	416.4 (126.9)	407.1 (124.1)	7.2 (2.2)	.6 (.2)	207.4 (9930)	198.4 (9500)	1.0	.1
7	9.1	8.2	10.8	341.8 (104.2)	328.8 (100.2)	9.9 (3.0)	1.3 (.4)	126.7 (6070)	117.3 (5620)	1.7	.2
8	9.3	8.0	11.4	384.6 (117.2)	374.8 (114.2)	12.8 (3.9)	1.0 (.3)	160.2 (7670)	152.1 (7280)	1.4	.2
9	9.4	12.0	14.8	341.3 (104.0)	336.8 (102.7)	6.2 (1.9)	.2 (.1)	120.6 (5770)	117.4 (5620)	1.0	0
10	10.0	6.5	10.2	314.5 (95.9)	299.0 (91.1)	5.0 (1.5)	2.2 (.7)	99.1 (4740)	89.0 (4260)	.9	.4

TABLE 7. – INITIAL AND FINAL VALUES OF SIGNIFICANT PARAMETERS MEASURED ON THE APPROACHES MADE IN THE F-104A AIRPLANE

Run	α, deg	Control-surface position, deg		V, ft/sec (m/sec)		$\dot{h}$, ft/sec (m/sec)		q, lb/ft^2 (N/m^2)		γ, deg	
		Initial	Final	Initial	Final	Initial	Final	Initial	Final	Initial	Final
1	3.0	3.9	4.1	483.7 (147.4)	477.1 (145.4)	16.4 (5.0)	1.3 (0.4)	263.1 (12,600)	256.0 (12,260)	1.9	0.2
2	3.8	3.8	3.7	449.2 (136.4)	448.3 (136.6)	19.3 (5.9)	3.3 (1.0)	238.8 (11,430)	237.8 (11,390)	2.5	.4
3	4.6	4.5	4.5	386.0 (117.7)	383.1 (116.8)	11.1 (3.4)	2.1 (.6)	174.2 (8,340)	171.6 (8,220)	1.7	.3
4	4.7	4.5	4.5	416.2 (126.9)	411.4 (125.4)	13.1 (4.0)	2.8 (.9)	194.4 (9,310)	190.1 (9,100)	1.8	.4
5	4.7	4.1	4.1	389.5 (118.7)	386.4 (117.8)	14.1 (4.3)	1.2 (.4)	170.2 (8,150)	167.5 (8,020)	2.1	.2
6	5.5	4.6	4.8	367.7 (112.1)	360.7 (109.9)	20.5 (6.3)	2.9 (.9)	158.0 (7,560)	151.9 (7,280)	3.2	.5
7	6.9	4.7	5.1	345.6 (105.3)	340.8 (103.9)	11.8 (3.6)	0 (0)	139.7 (6,690)	135.8 (6,500)	2.0	0
8	7.5	5.0	5.0	338.2 (103.1)	337.1 (102.7)	13.1 (4.0)	9.3 (2.9)	131.0 (6,270)	130.1 (6,230)	2.2	1.6
9	8.0	6.0	6.8	341.8 (104.2)	340.4 (103.8)	9.4 (2.9)	0 (0)	133.1 (6,370)	132.0 (6,320)	1.6	0
10	9.3	5.8	6.9	325.6 (99.2)	320.0 (97.5)	14.4 (4.4)	1.7 (.5)	119.1 (5,700)	115.0 (5,510)	2.5	.3

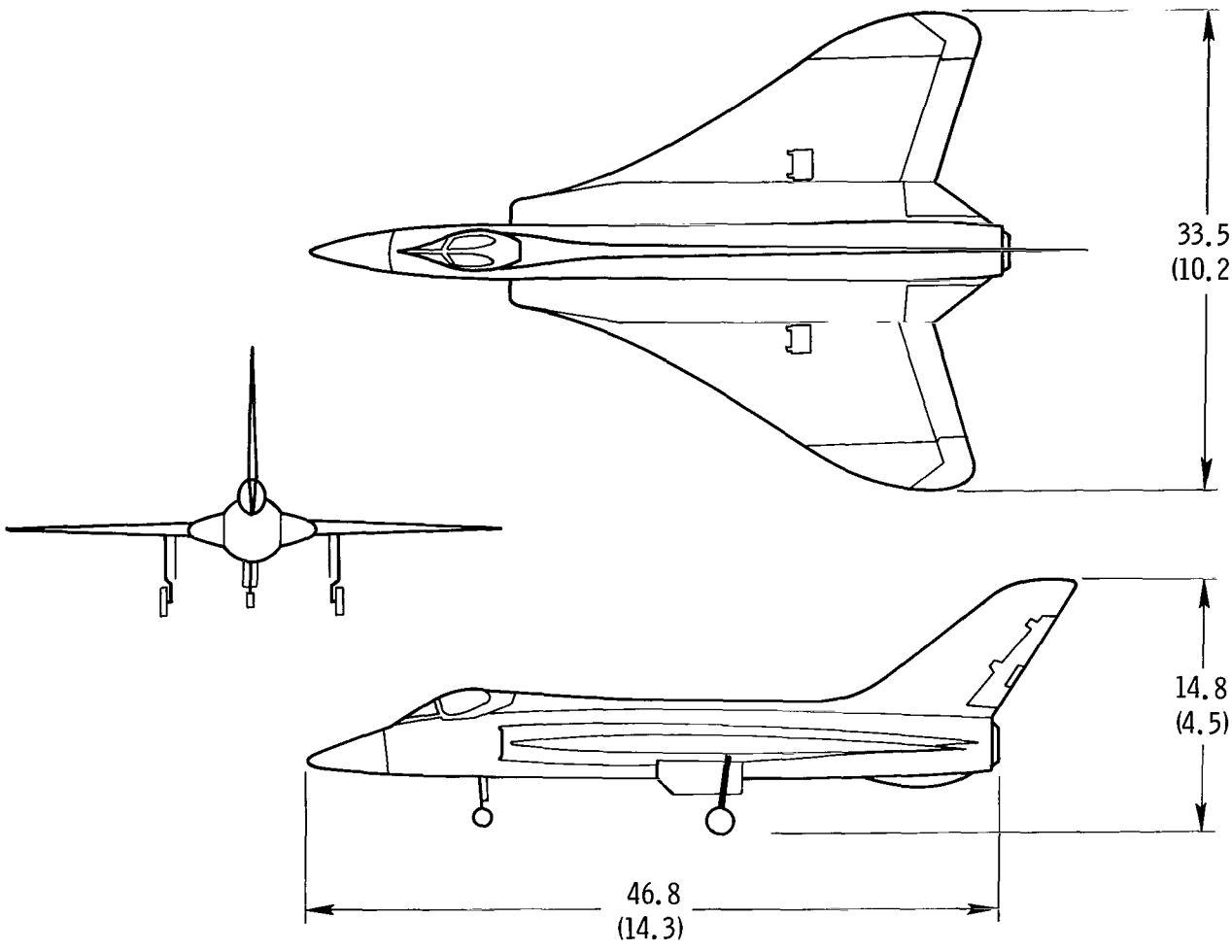

Figure 1. Three-view drawing of the F5D-1 airplane modified with an ogee wing. Dimensions in feet (meters).

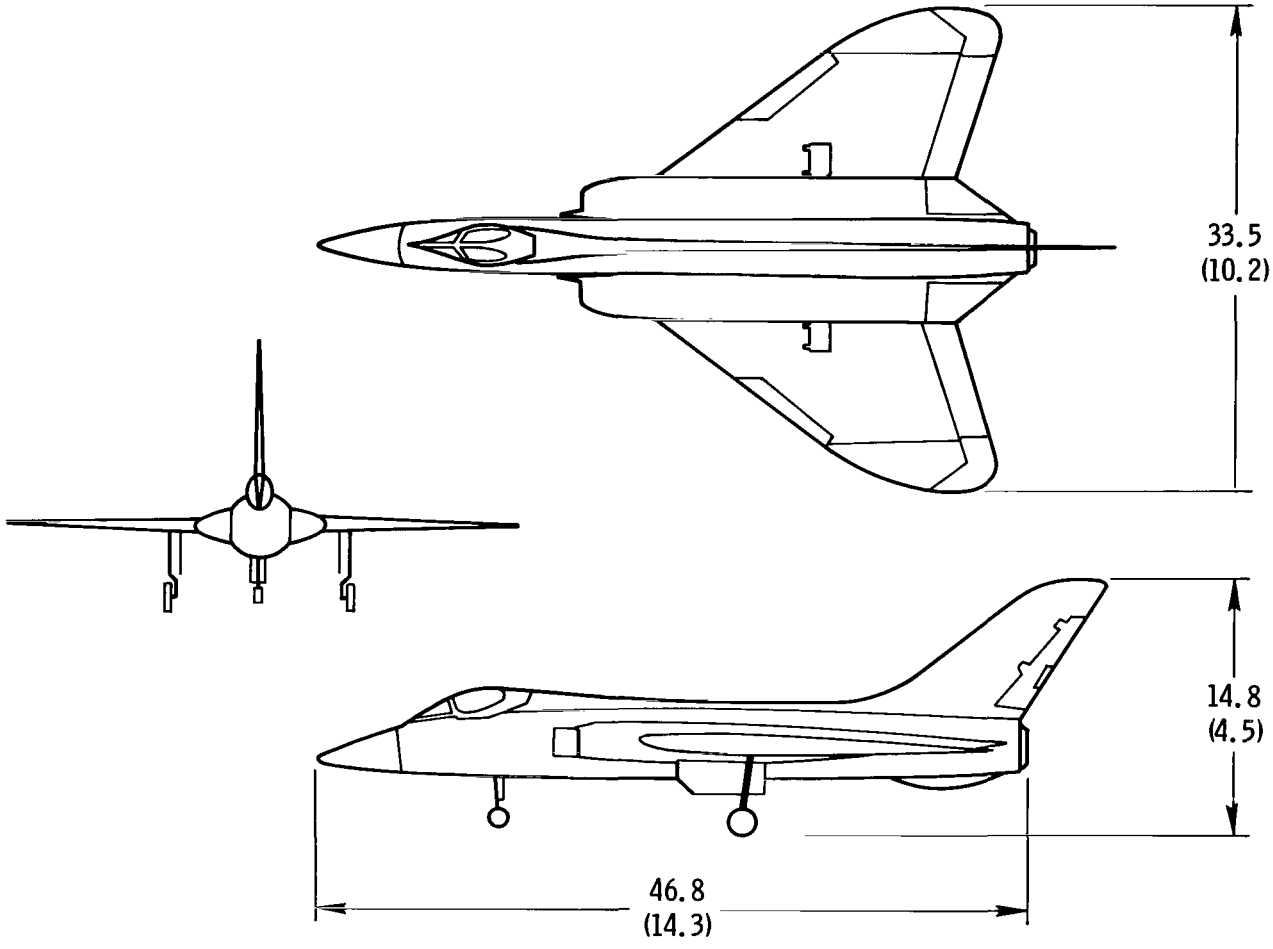

Figure 2. Three-view drawing of the basic F5D-1 airplane. Dimensions in feet (meters).

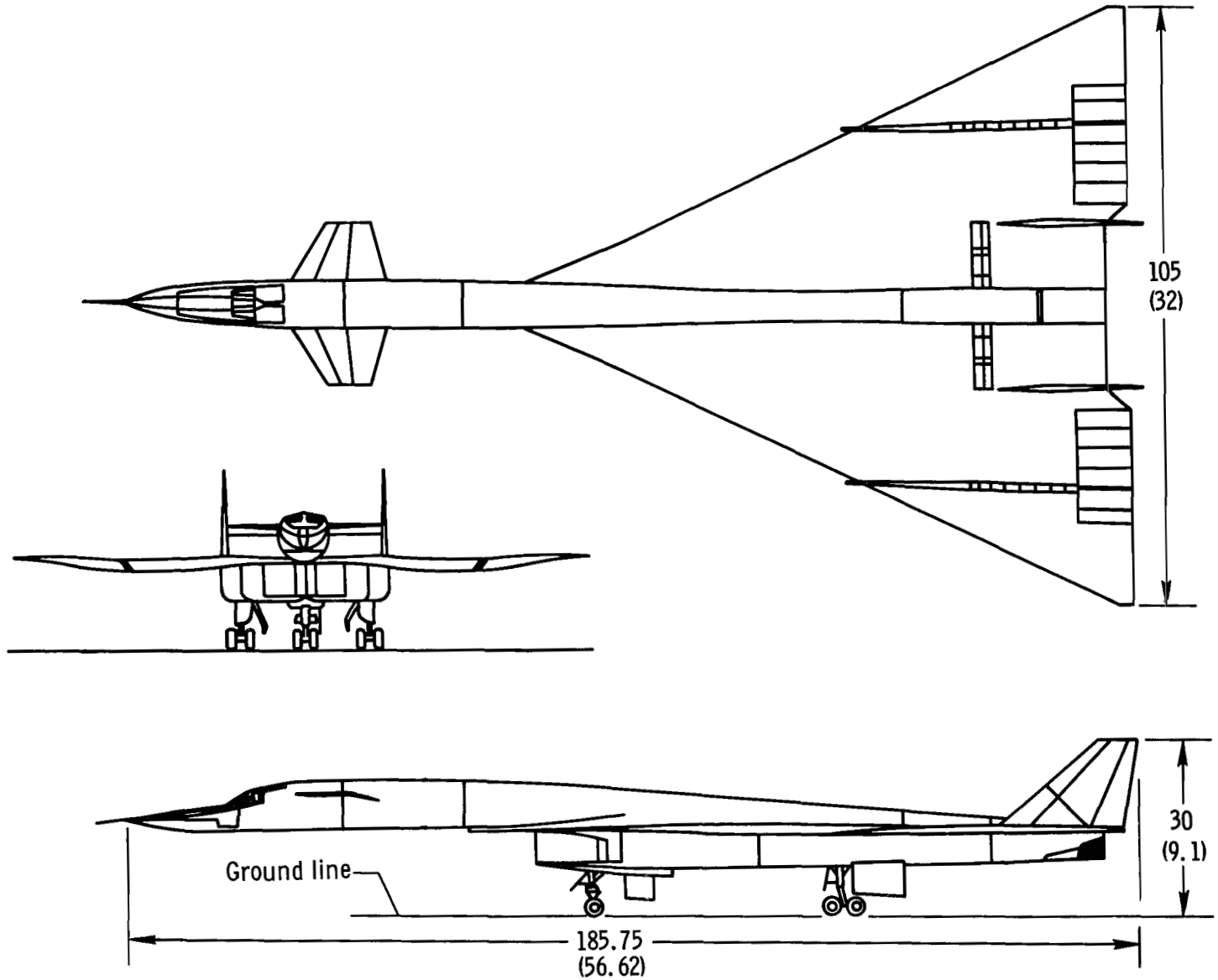

Figure 3. Three-view drawing of the XB-70 airplane. Dimensions in feet (meters).

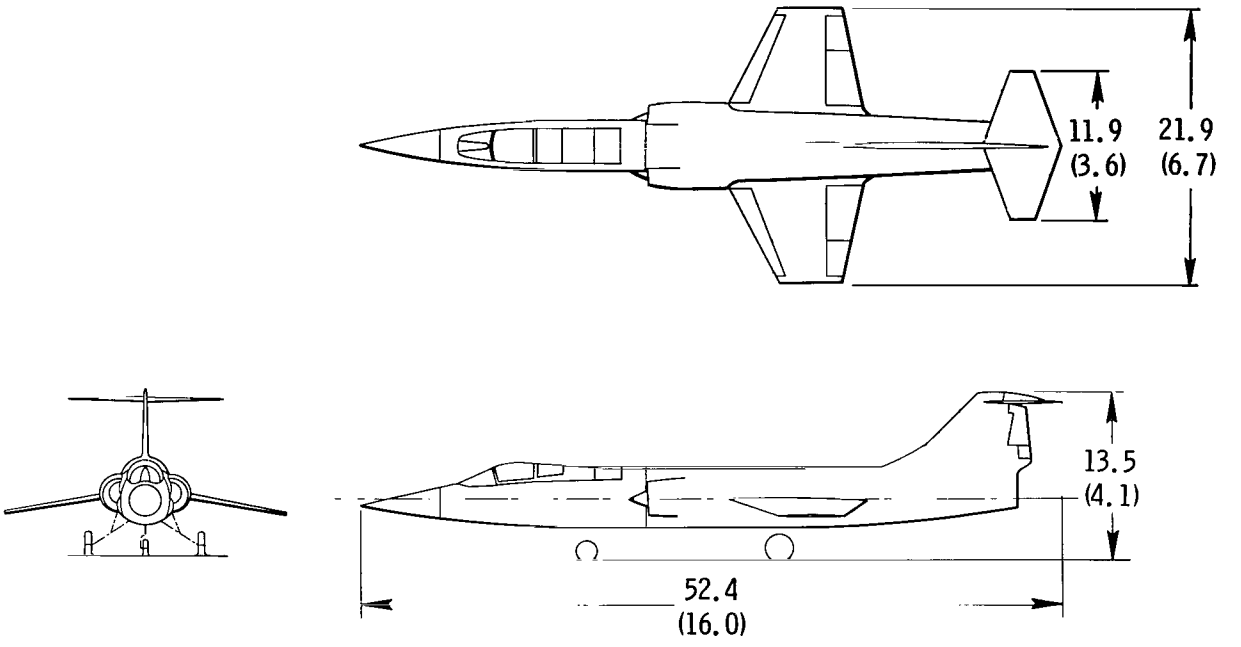

Figure 4. Three-view drawing of the F-104A airplane. Dimensions in feet (meters).

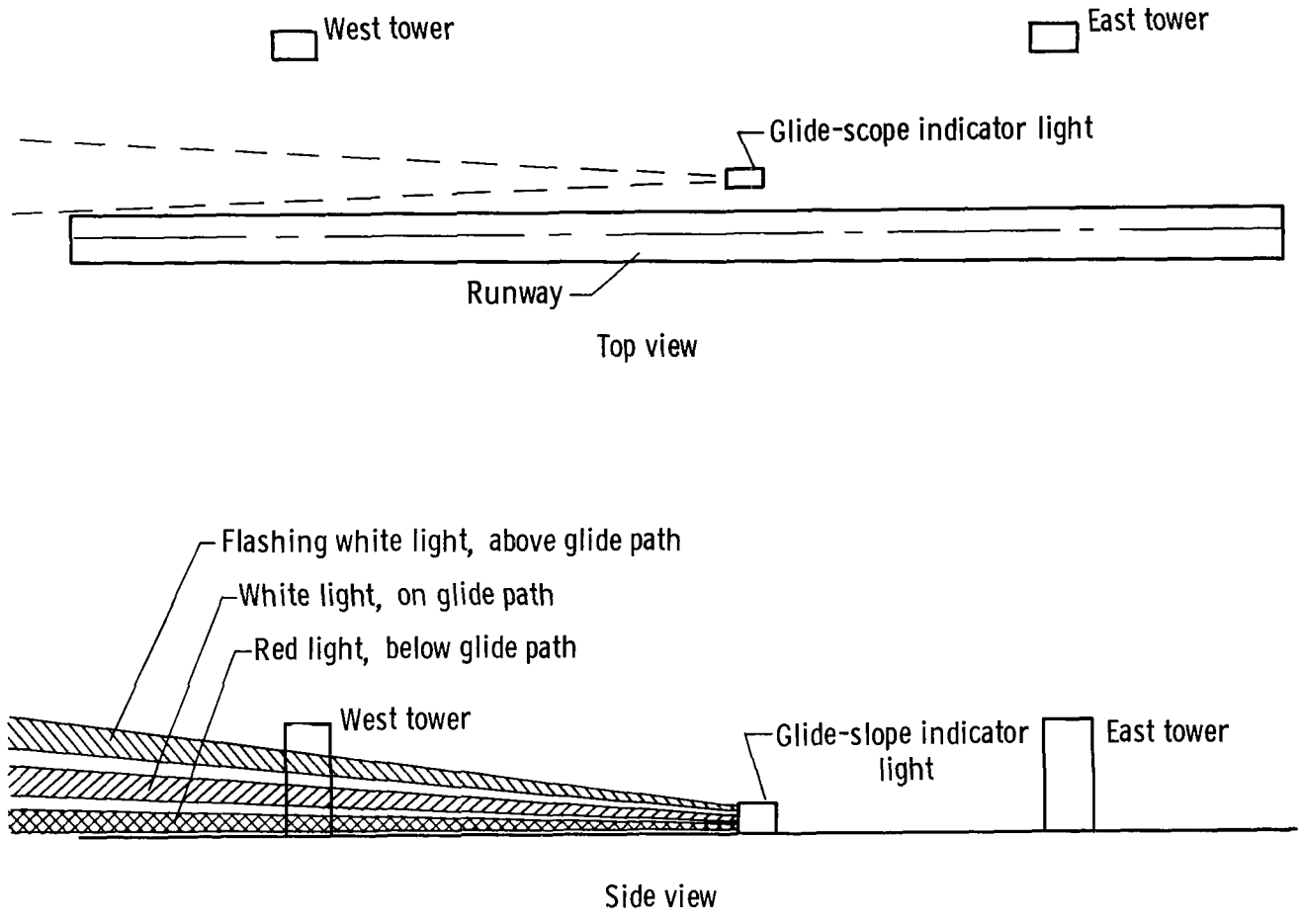

Figure 5. Two-view sketch of the glide-slope indicator light.

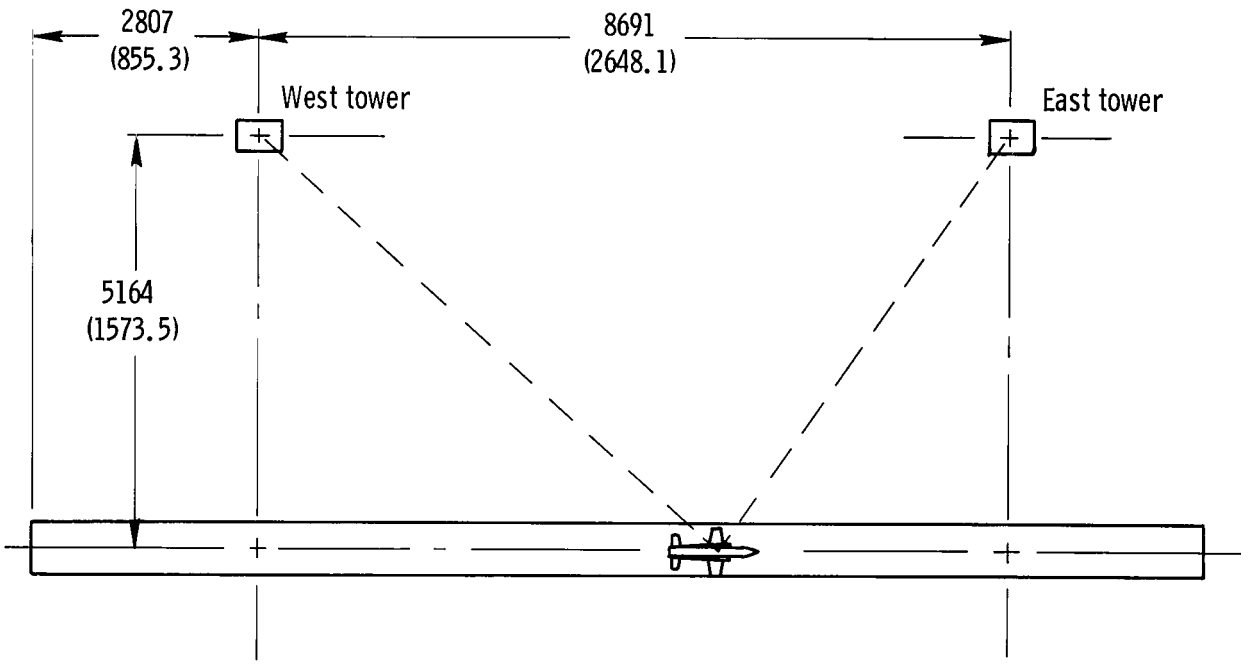

Figure 6. Sketch of the Air Force Flight Test Center runway tracking system. Dimensions in feet (meters).

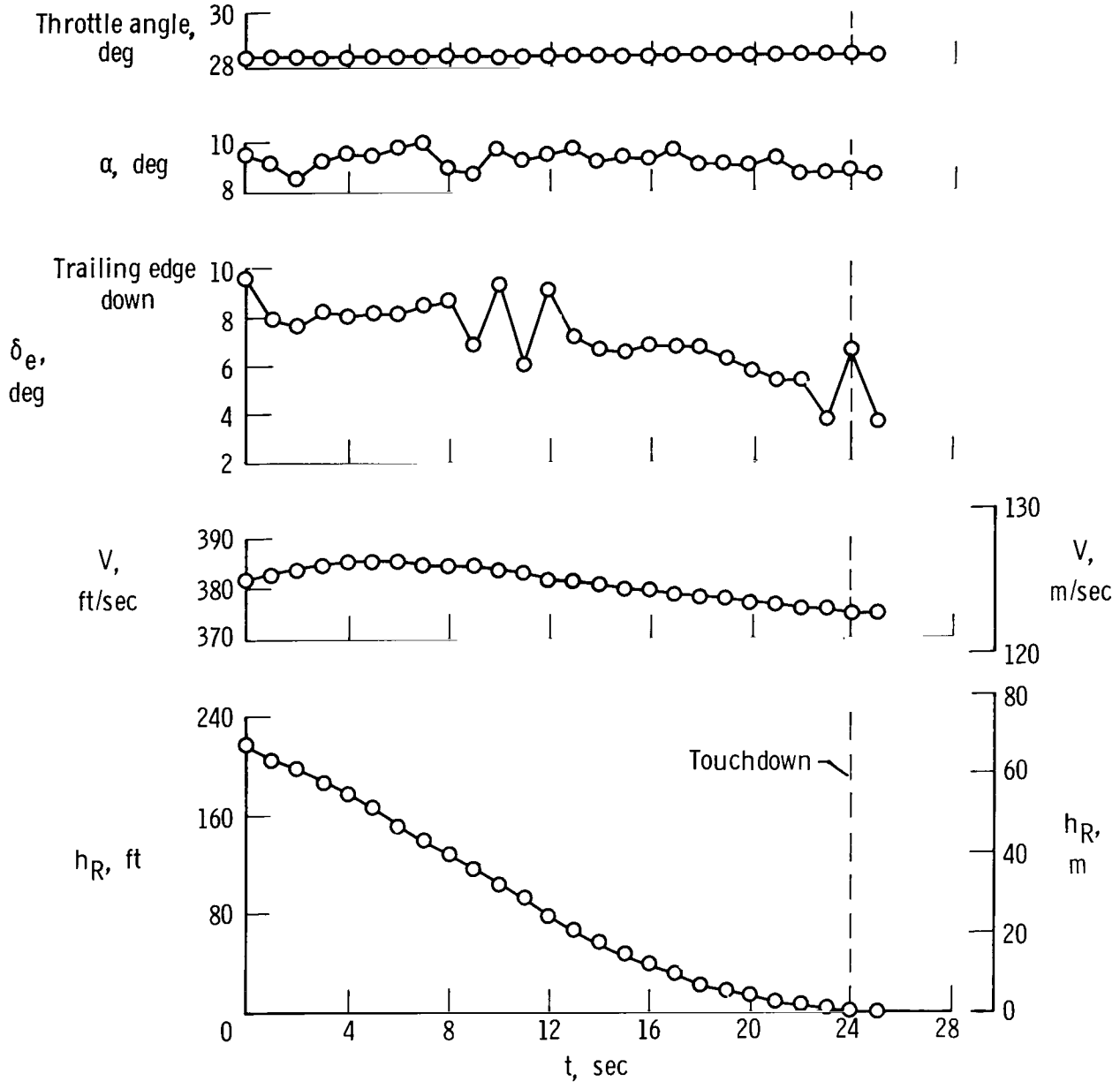

Figure 7. Time history of a constant-angle-of-attack approach in the XB-70-1 airplane.

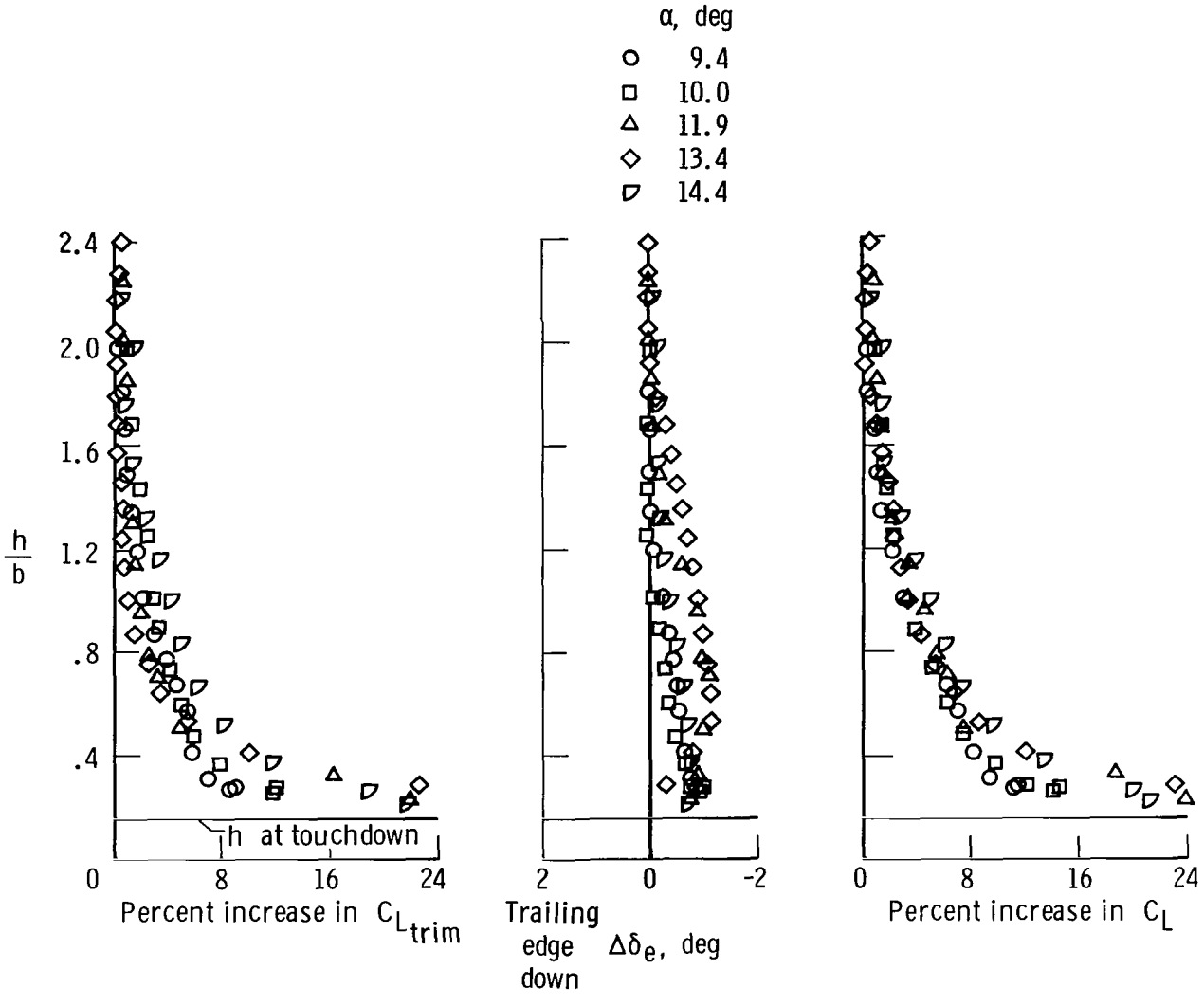

Figure 8. Effect of ground proximity on lift and pitching moment of the F5D-1 airplane modified with an ogee wing.

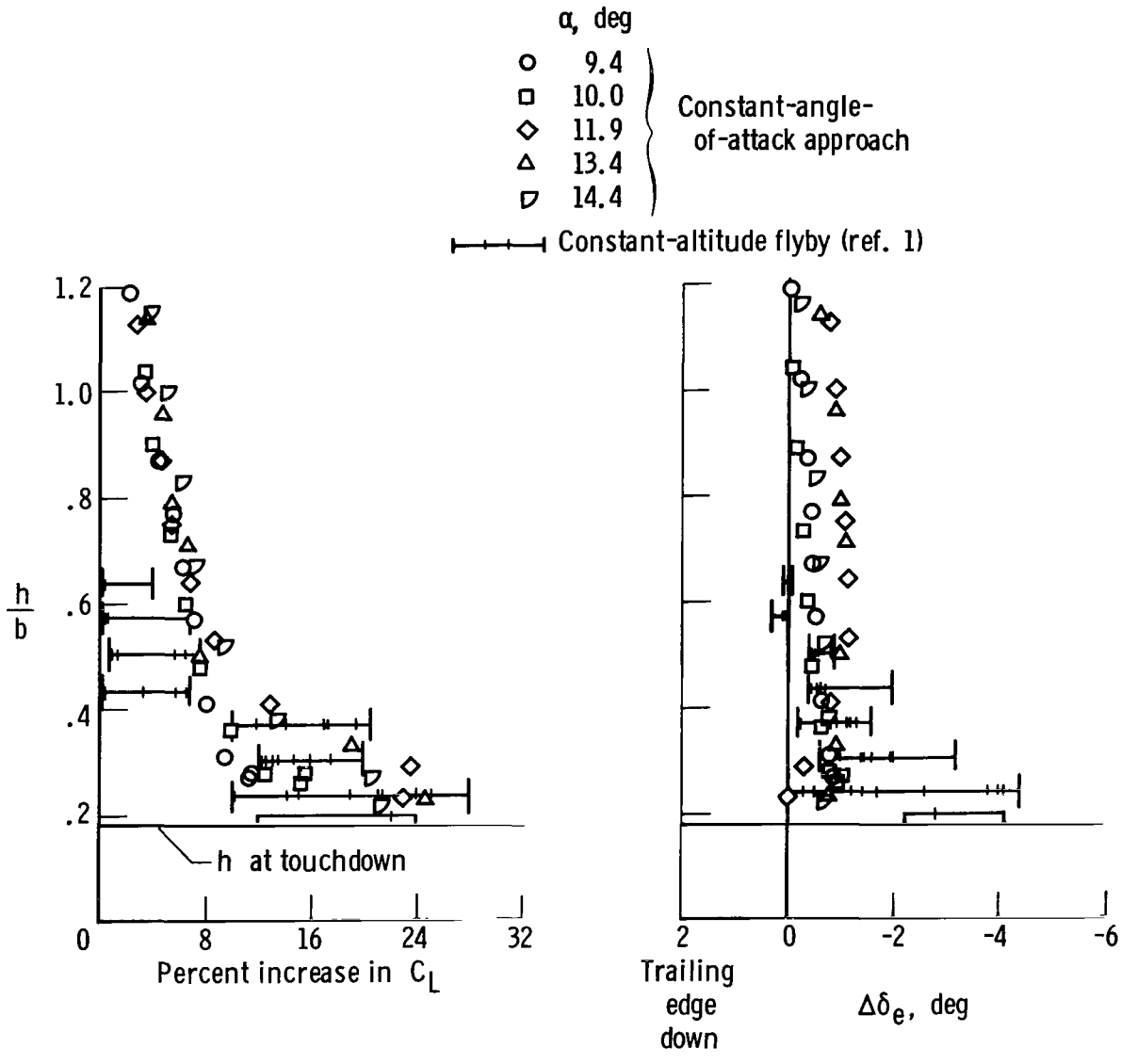

Figure 9. Comparison of constant-angle-of-attack and constant-altitude-flyby flight data for the modified F5D-1 airplane.

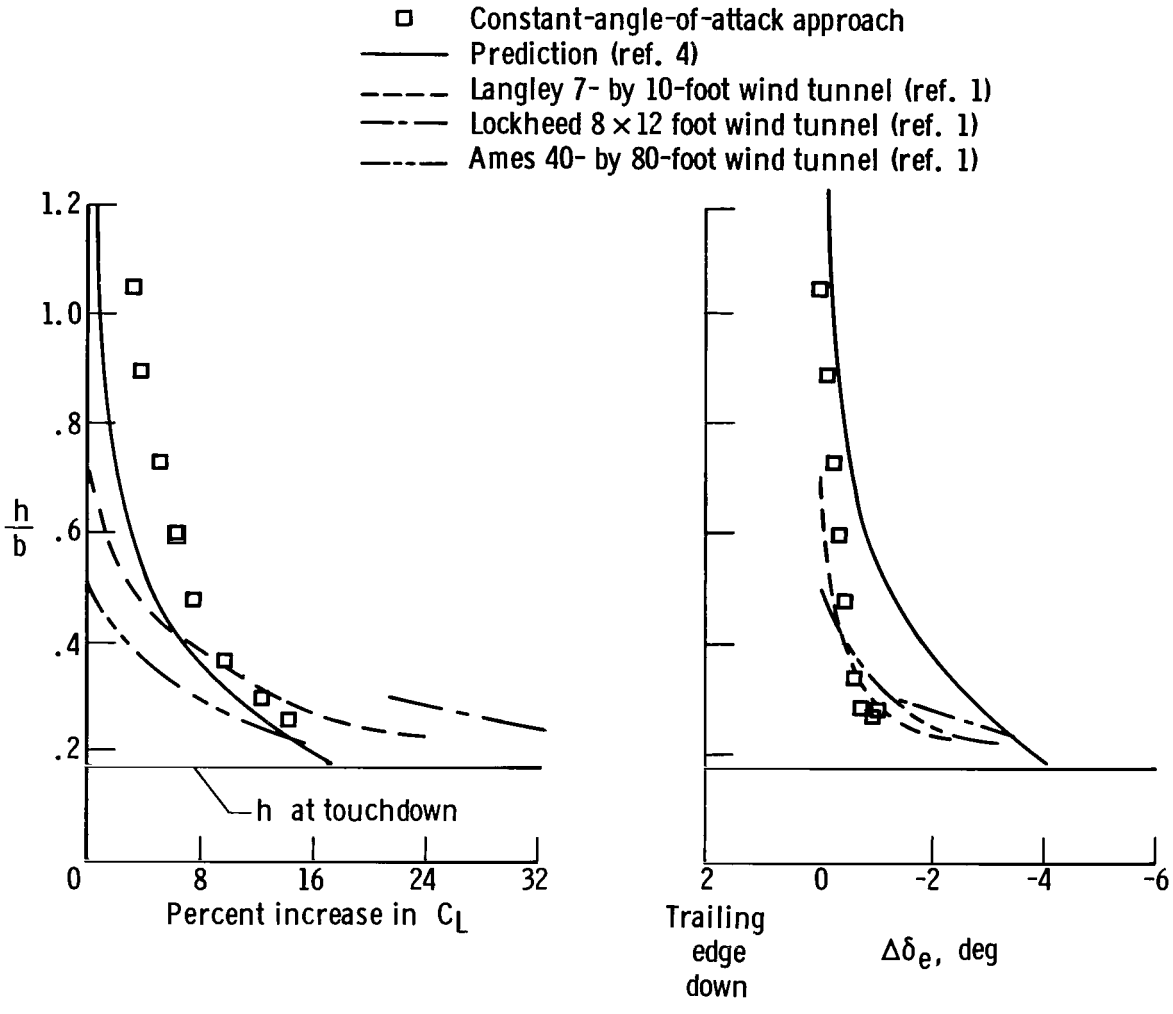

Figure 10. Comparison of flight, wind-tunnel, and theoretical ground-effect data for the modified F5D-1 airplane at 10° angle of attack.

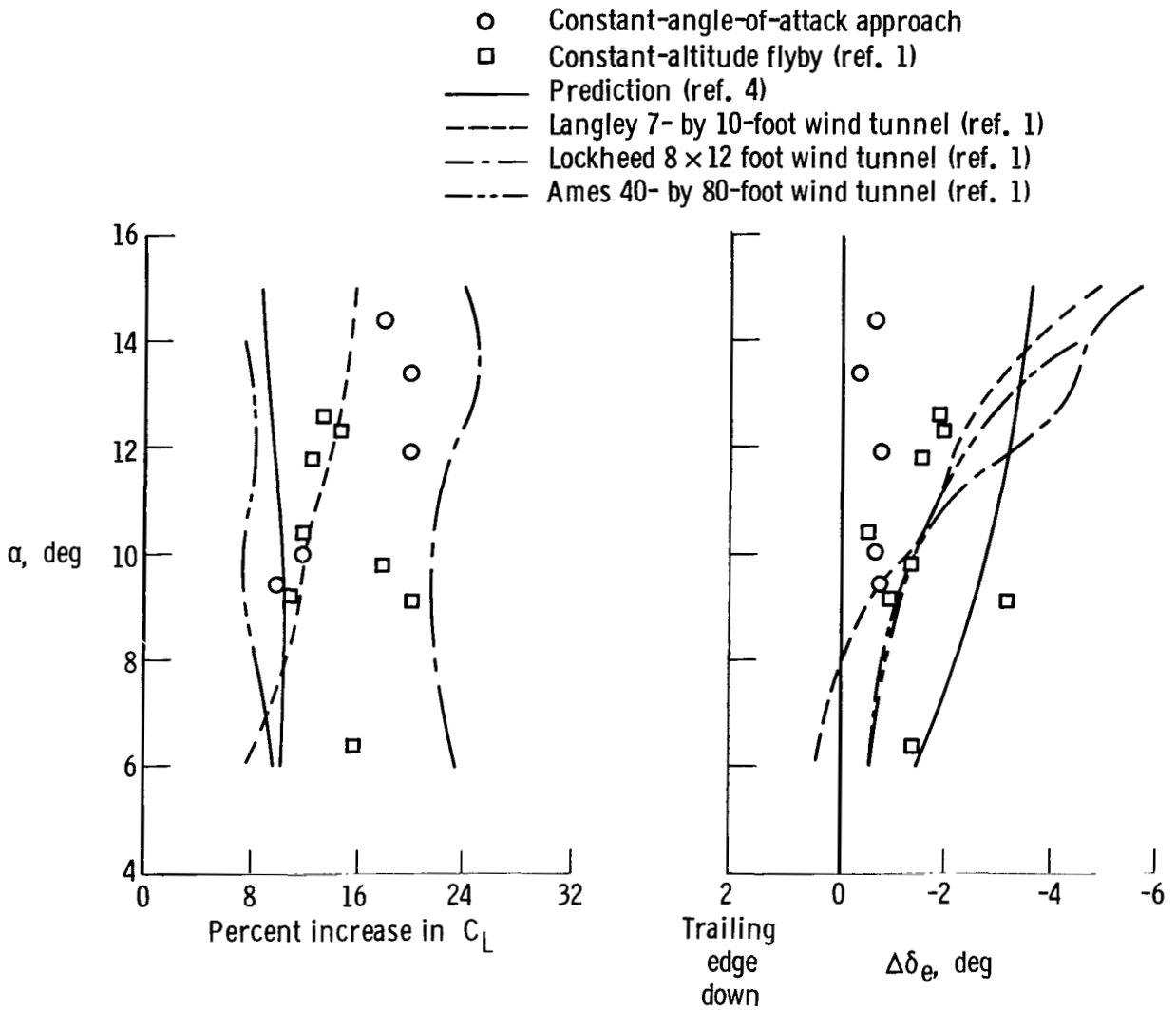

Figure 11. Variation of incremental lift coefficient and elevon deflection with angle of attack for flight, wind-tunnel, and theoretical ground-effect data on the modified F5D-1 airplane at $h/b = 0.30$.

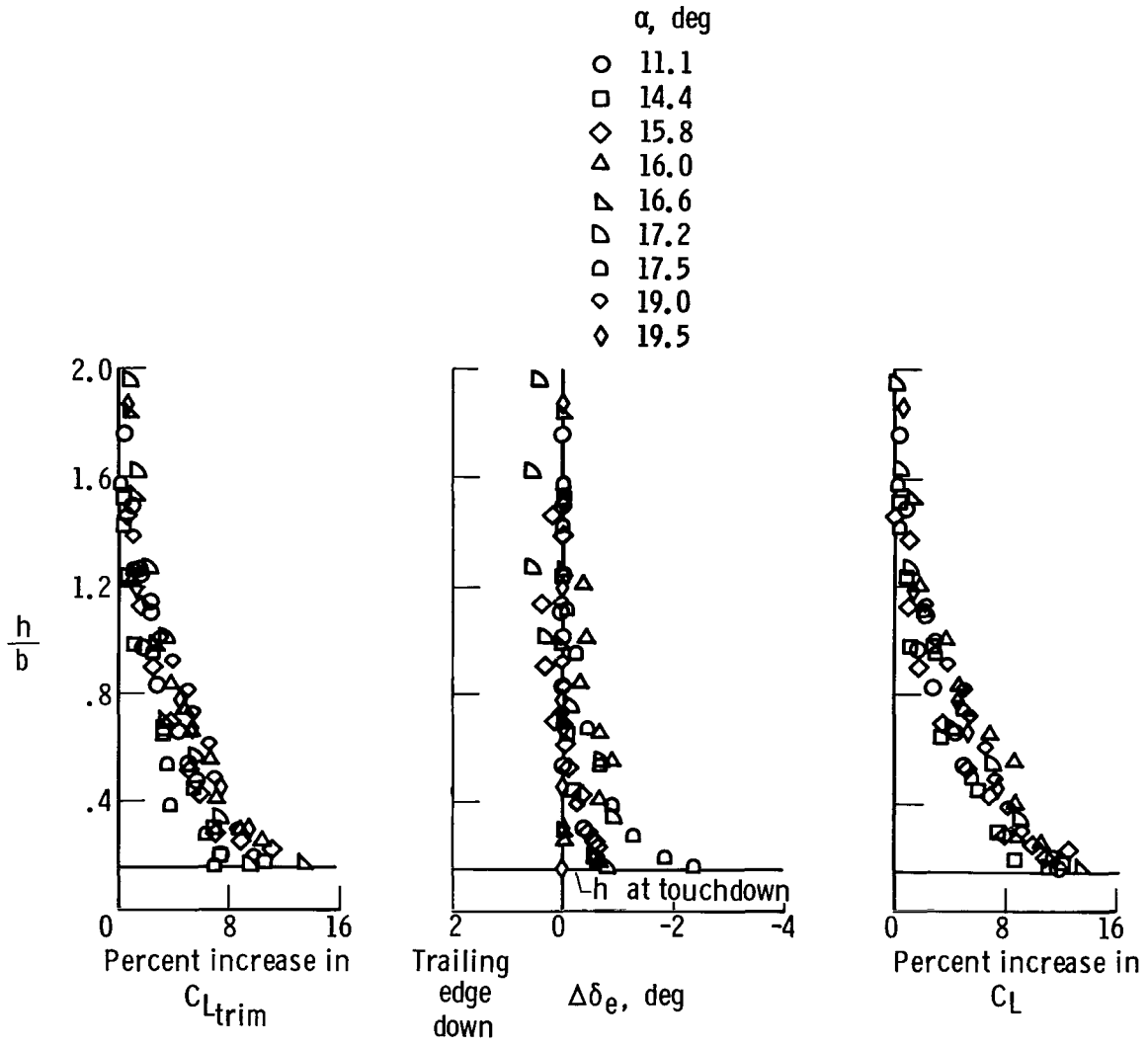

Figure 12. Effect of ground proximity on lift coefficient and elevon deflection of the basic F5D-1 airplane.

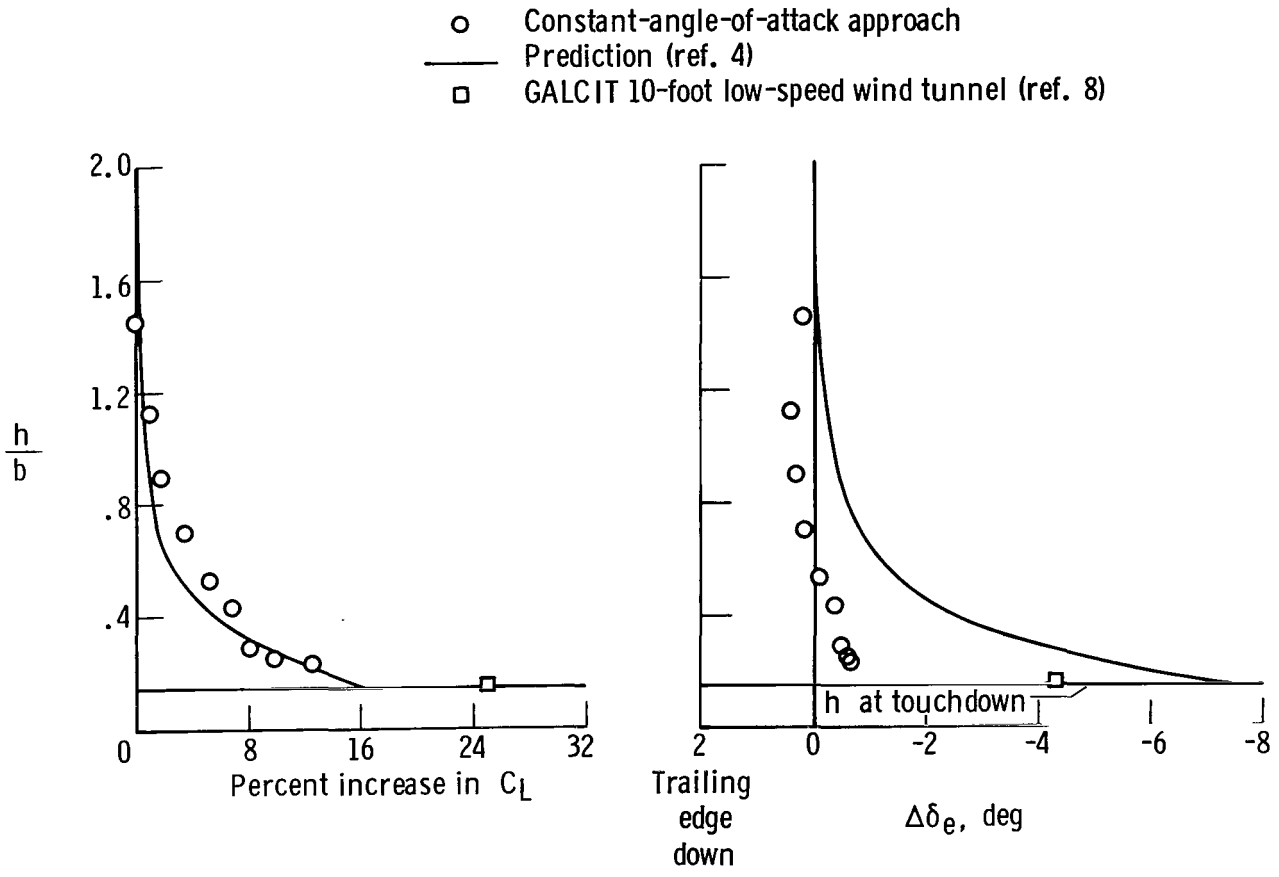

Figure 13. Comparison of flight, wind-tunnel, and theoretical ground-effect data for the basic F5D-1 airplane at 15.8° angle of attack.

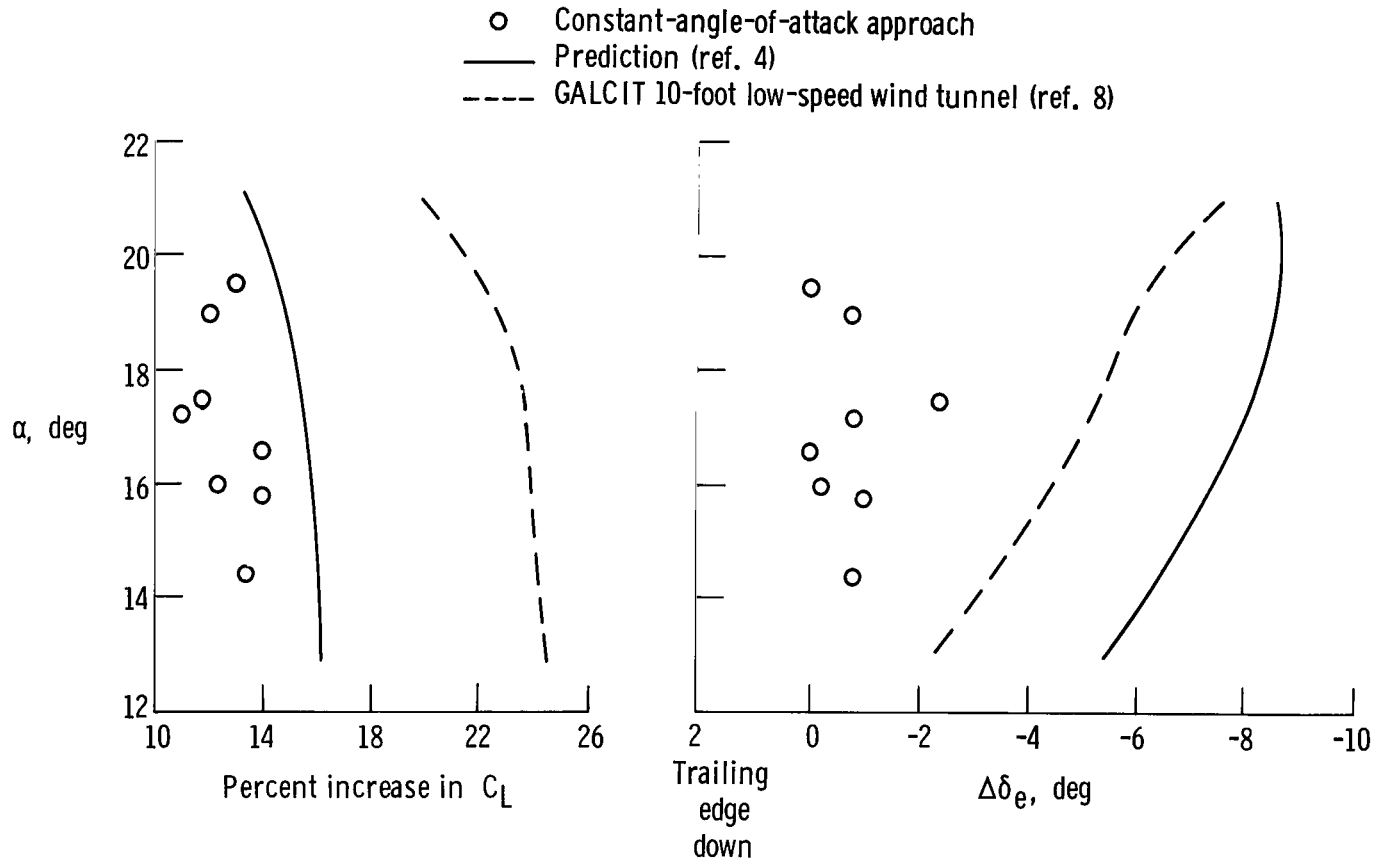

Figure 14. Variation of incremental lift coefficient and elevon deflection with angle of attack for flight, wind-tunnel, and theoretical ground-effect data on the basic F5D-1 airplane at h/b = 0.16.

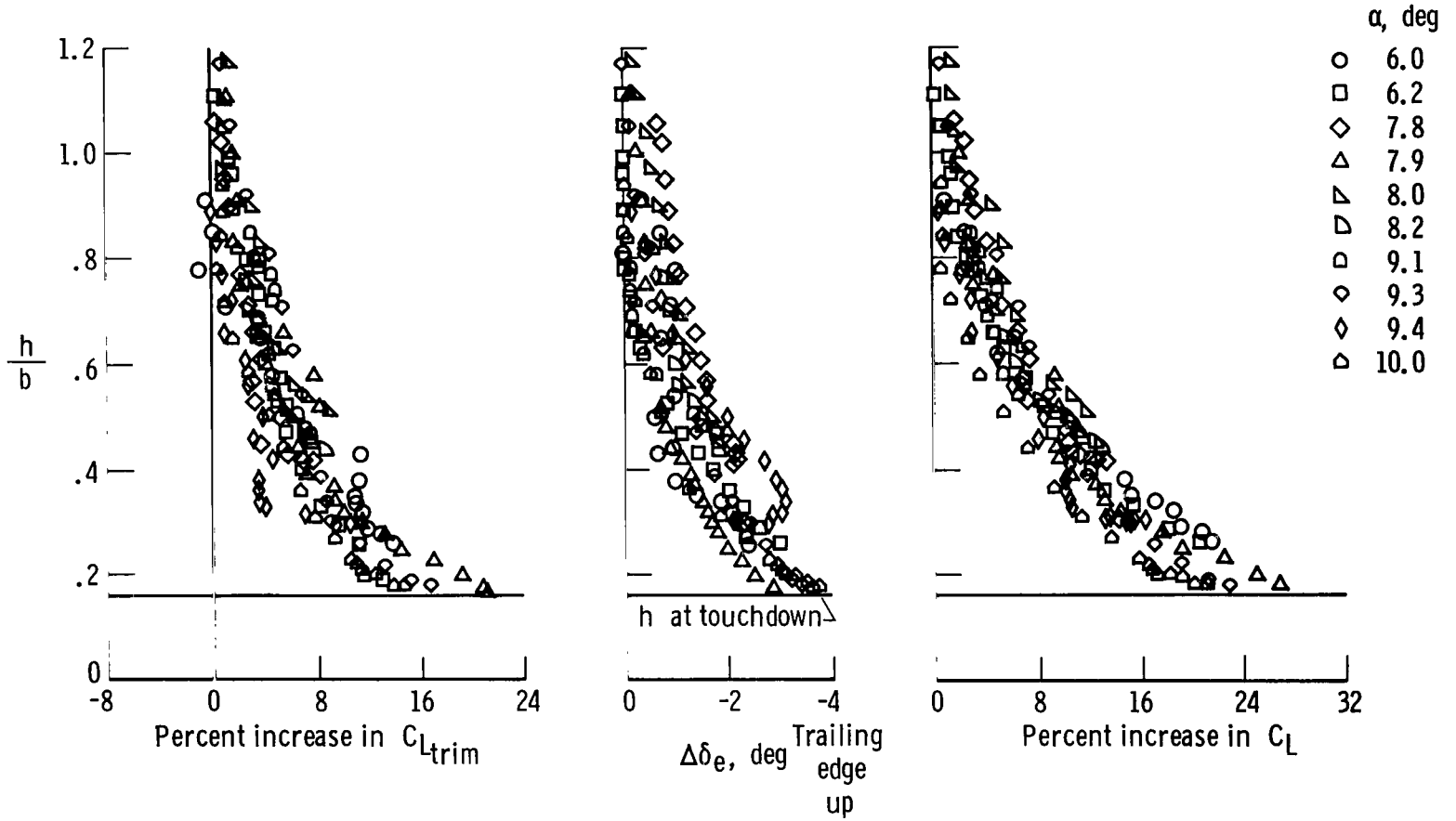

Figure 15. Effect of ground proximity on lift and pitching moment of the XB-70 airplanes.

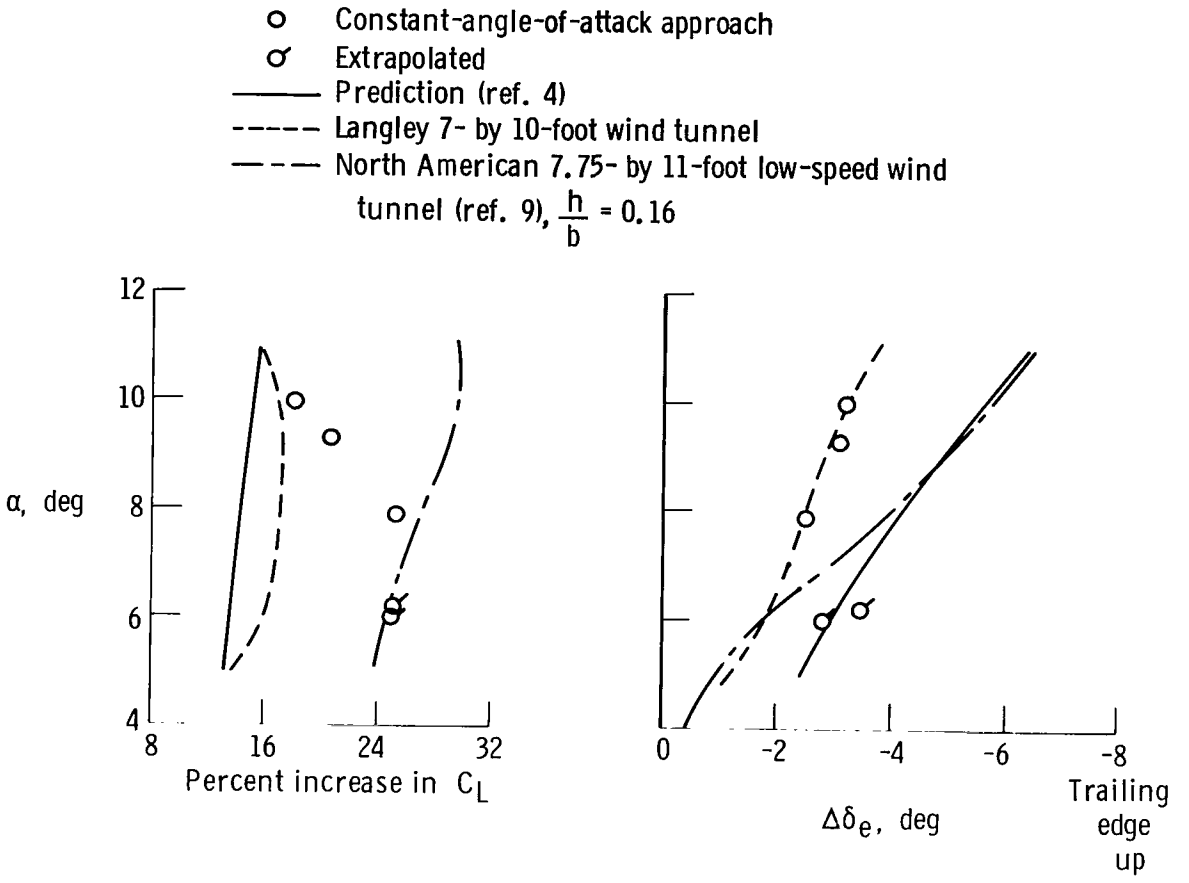

Figure 16. Variation of incremental lift coefficient and elevon deflection with angle of attack for flight, wind-tunnel, and theoretical ground-effect data on the XB-70 airplanes at h/b = 0.20.

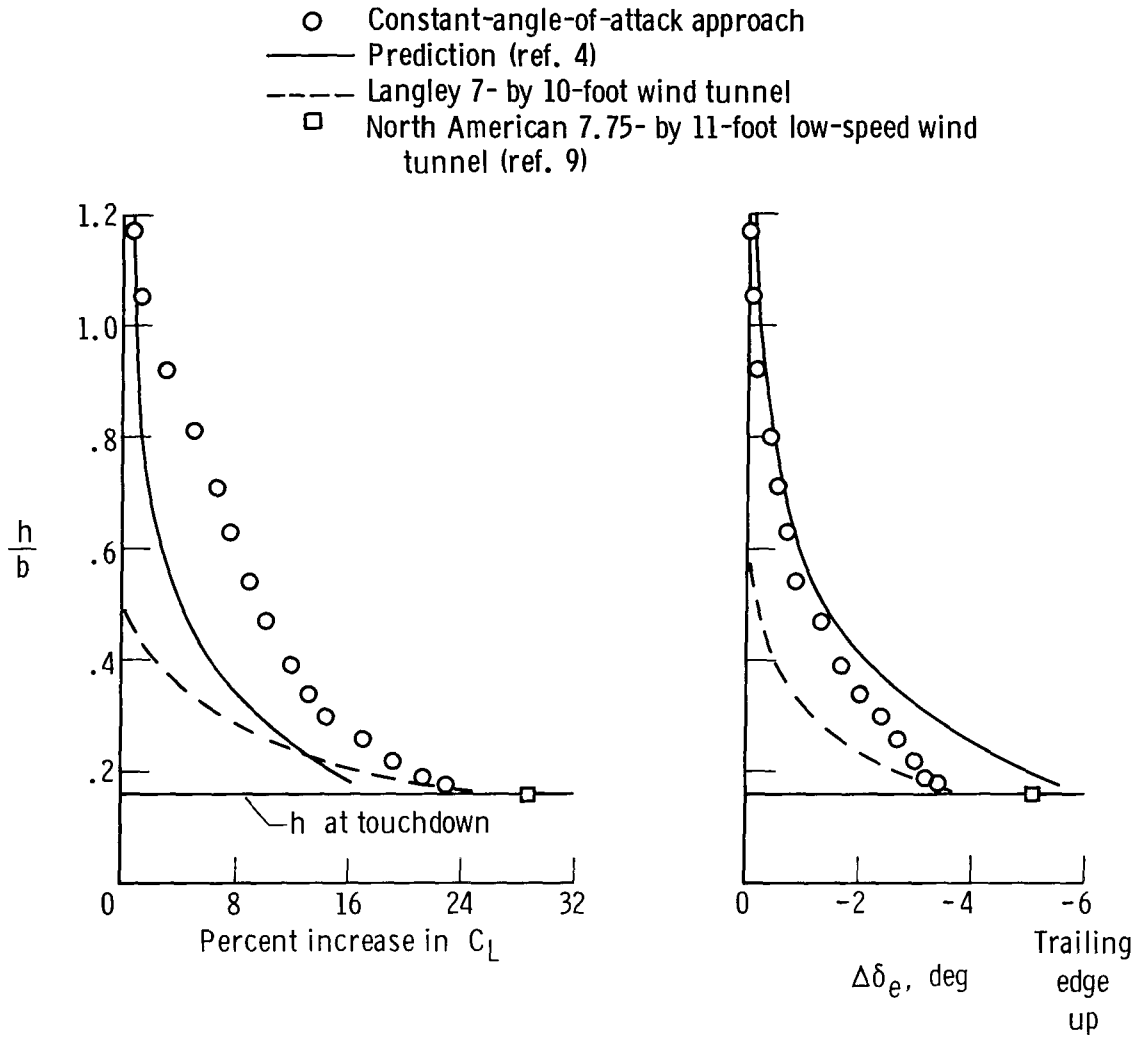

Figure 17. Comparison of flight, wind-tunnel, and theoretical ground-effect data for the XB-70 airplanes at 9.3° angle of attack.

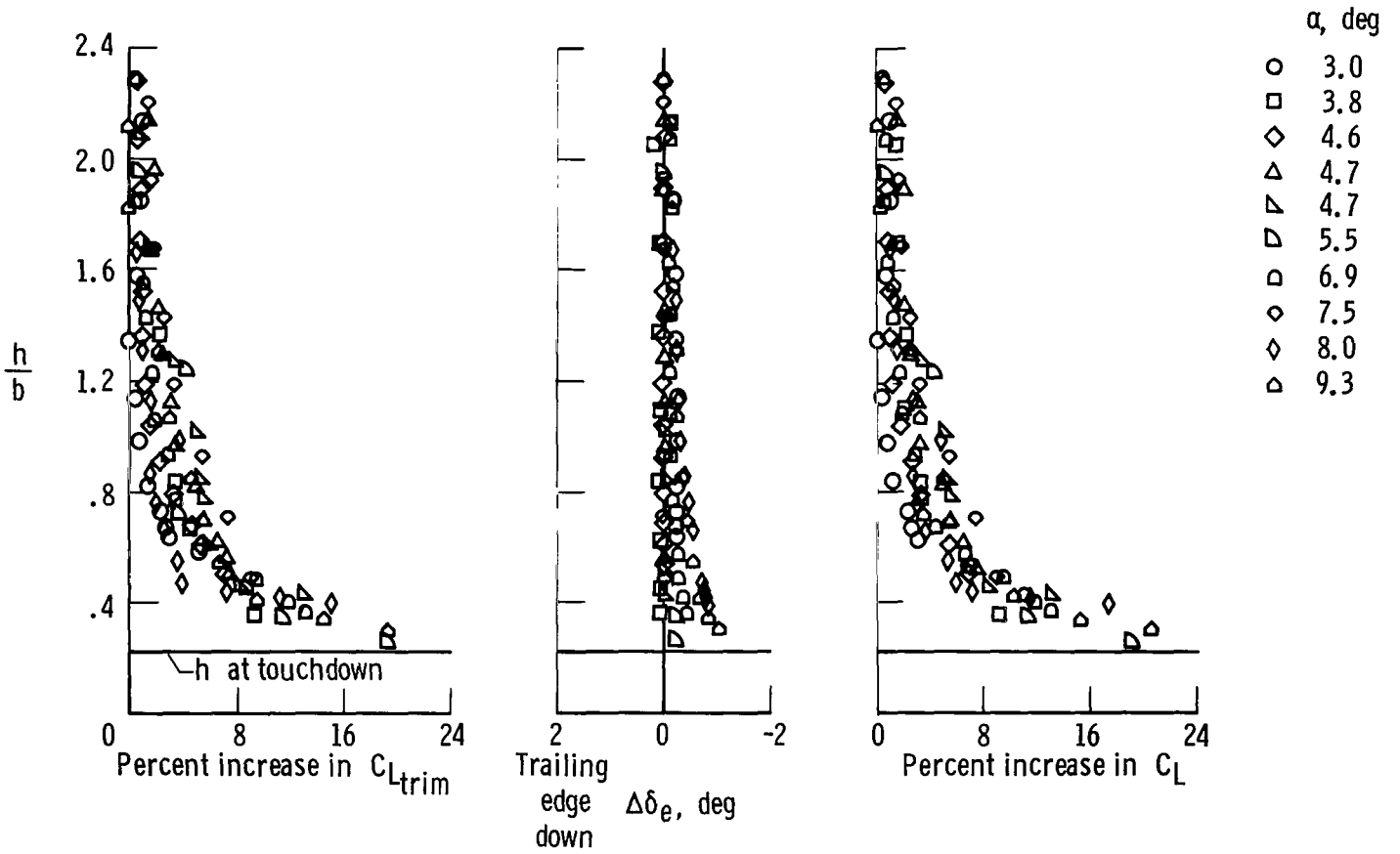

Figure 18. Effect of ground proximity on lift and pitching moment of the F-104A airplane.

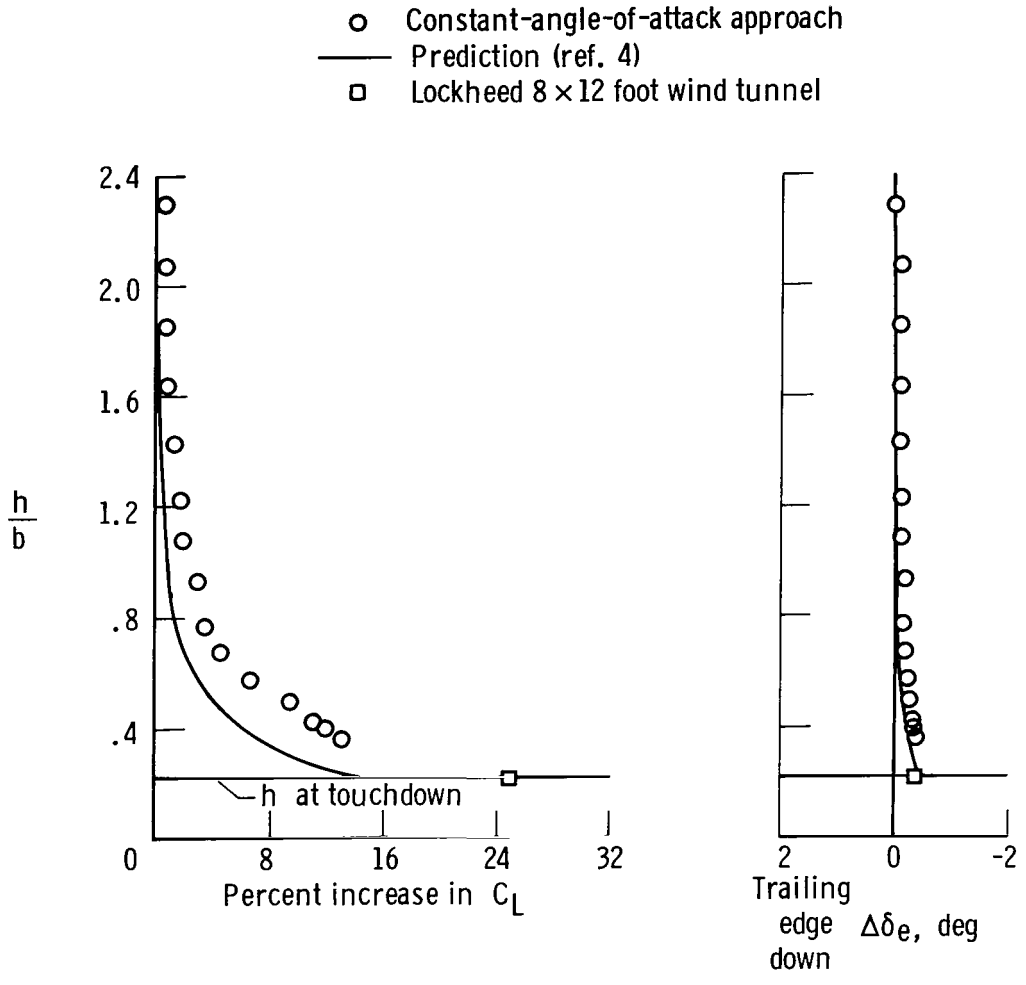

Figure 19. Comparison of flight, wind-tunnel, and theoretical ground-effect data for the F-104A airplane at 6.9° angle of attack.

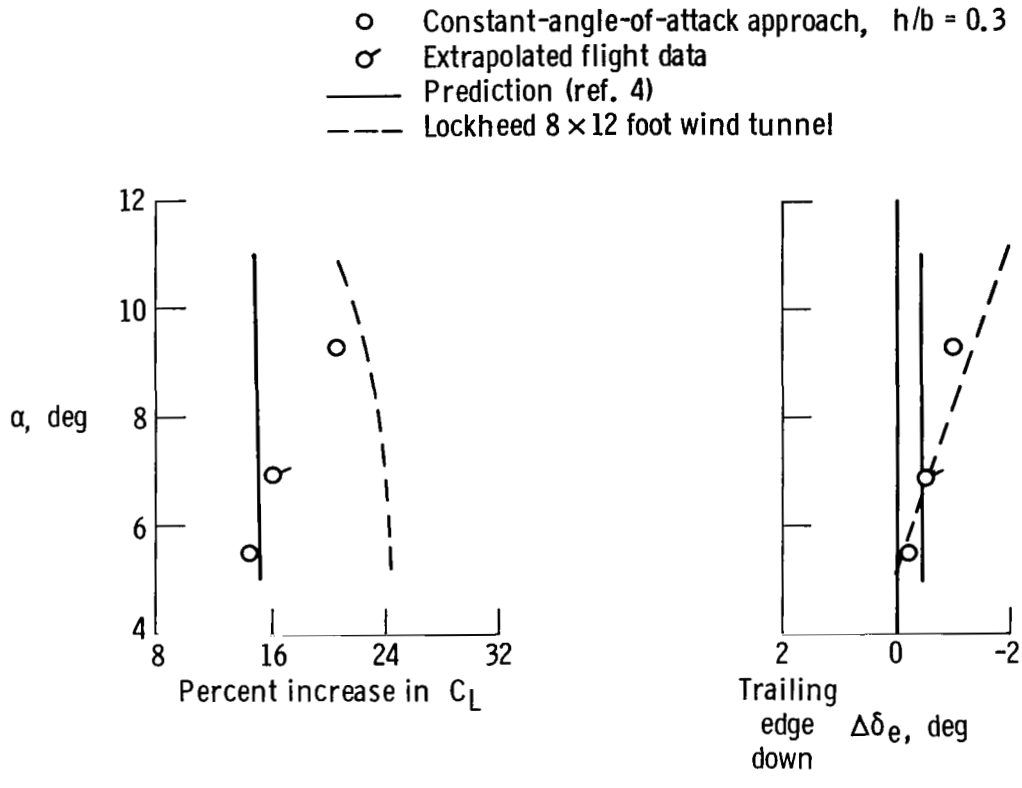

Figure 20. Variation of incremental lift coefficient and elevon deflection with angle of attack for flight, wind-tunnel, and theoretical ground-effect data on the F-104A airplane at h/b = 0.22.

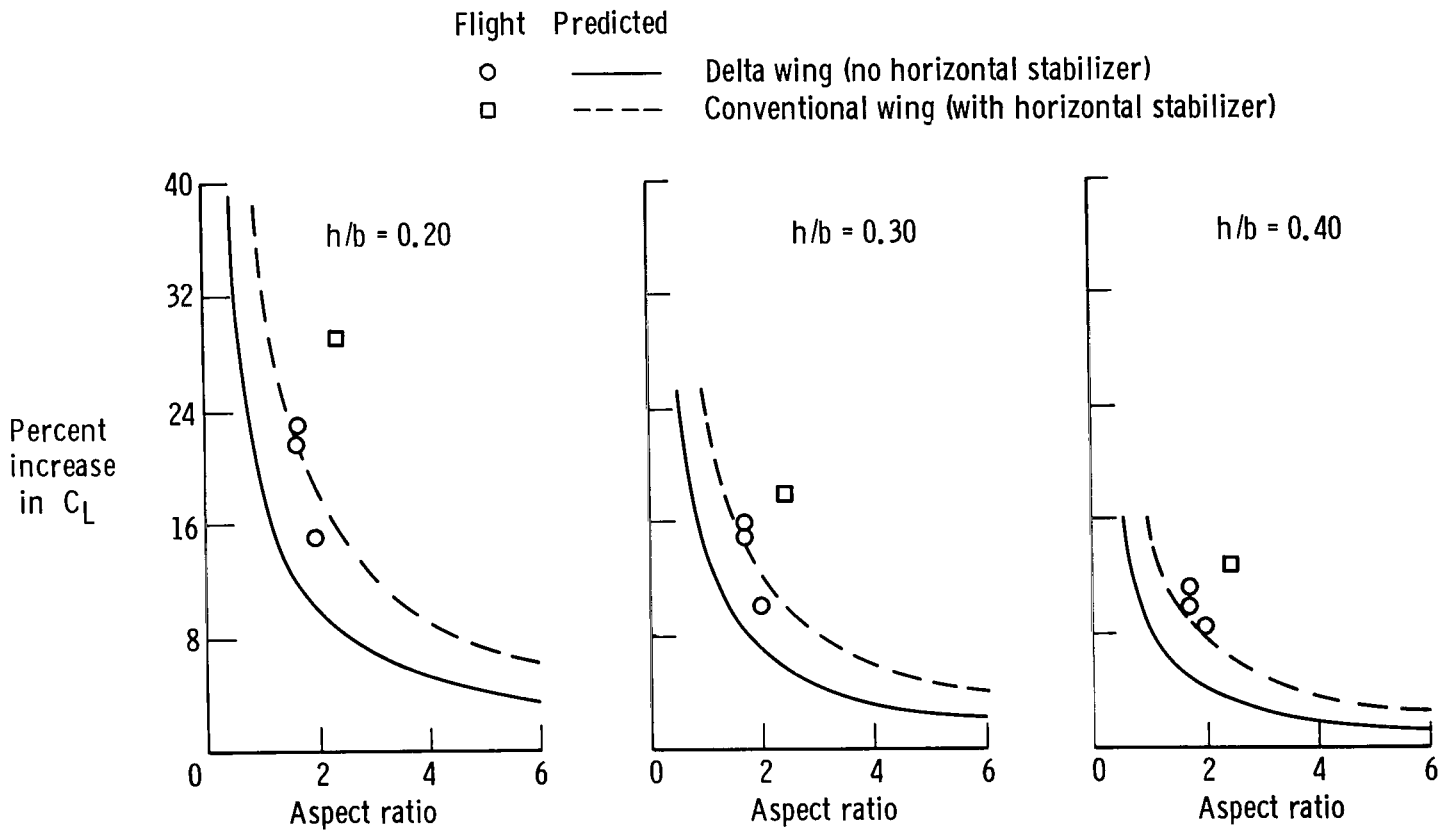

Figure 21. Variation of lift coefficient with aspect ratio for flight and theoretical ground-effect data.

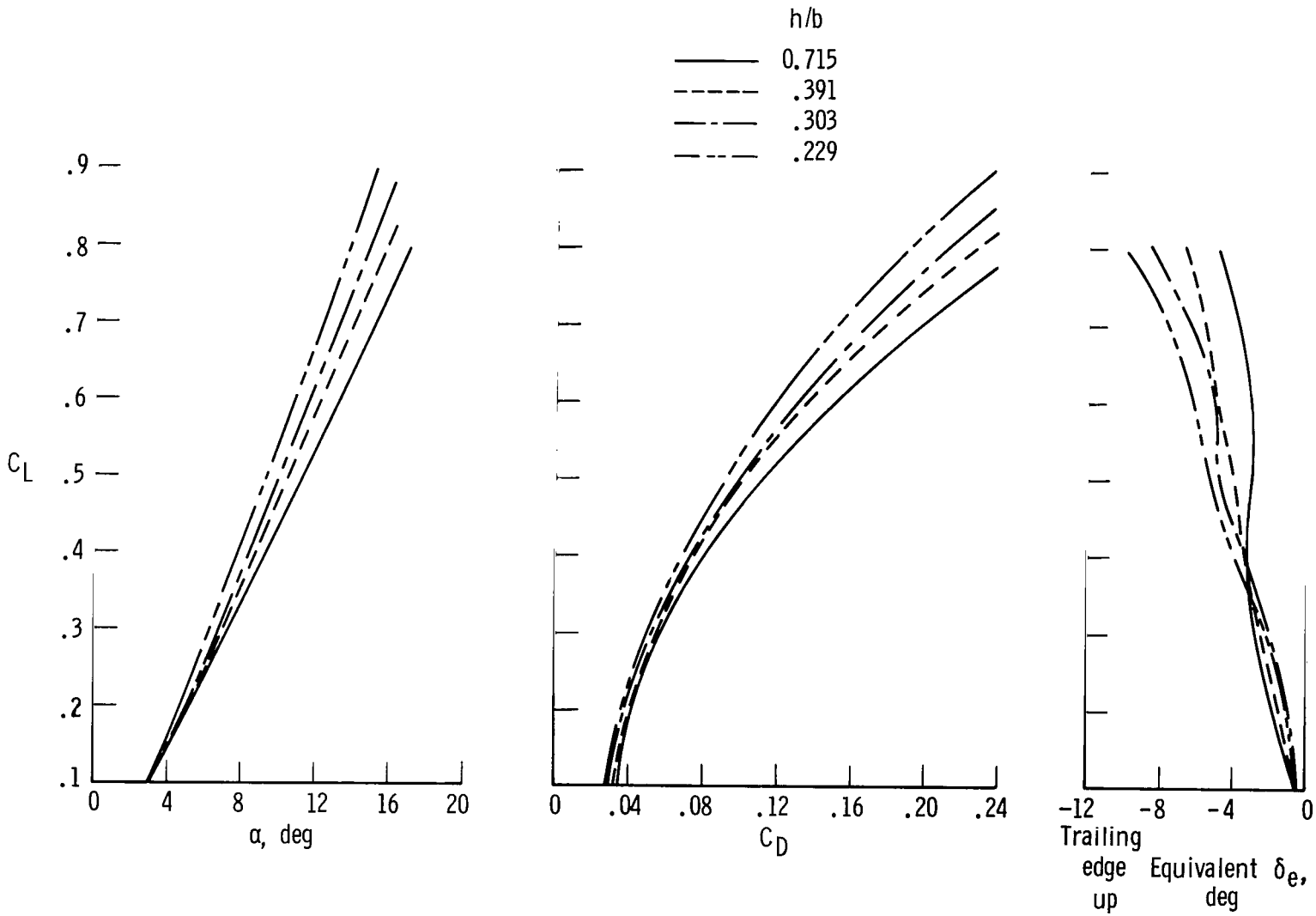

Figure 22. Basic wind-tunnel data for the F5D-1 airplane modified with an ogee wing (ref. 1).

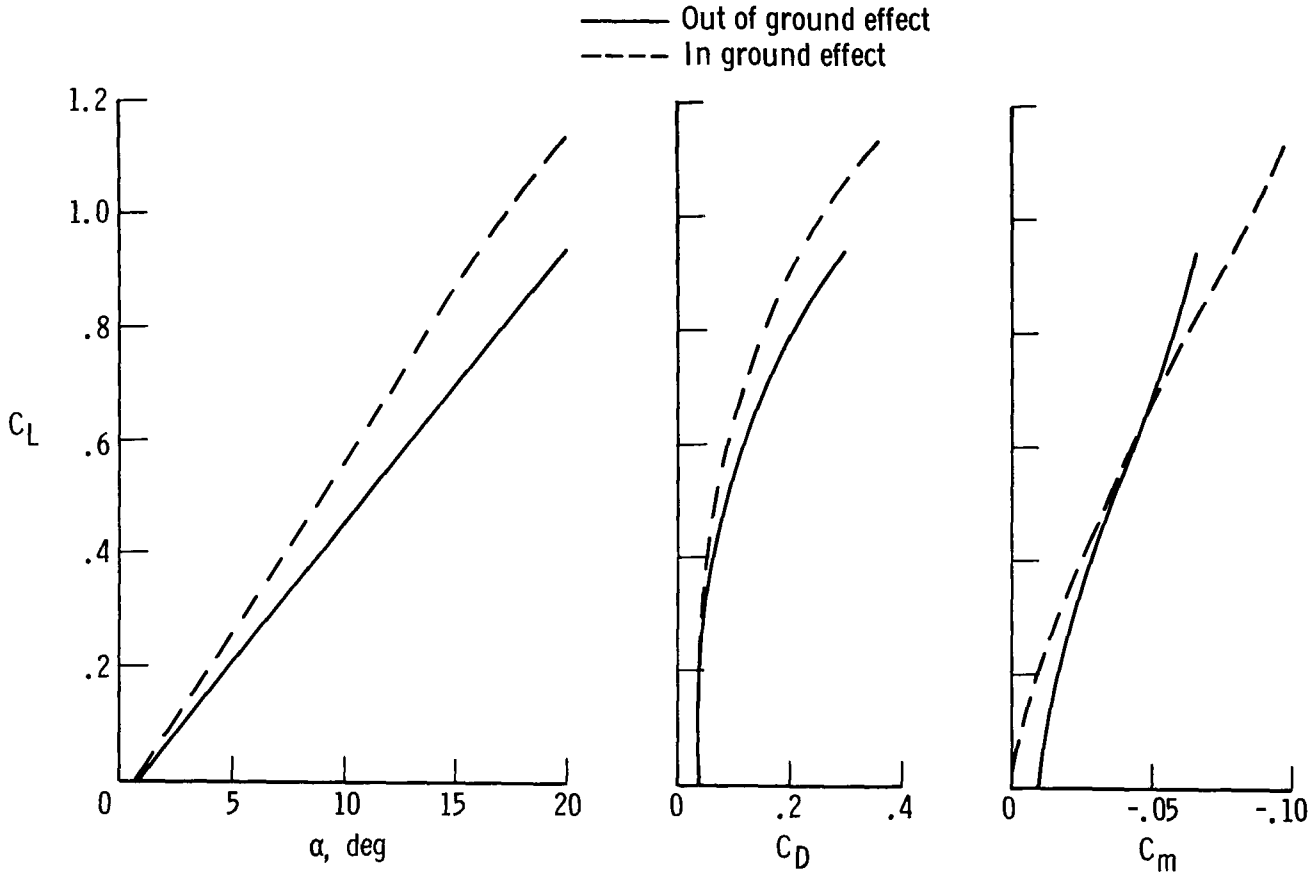

Figure 23. Basic wind-tunnel data for the basic F5D-1 airplane (ref. 8).

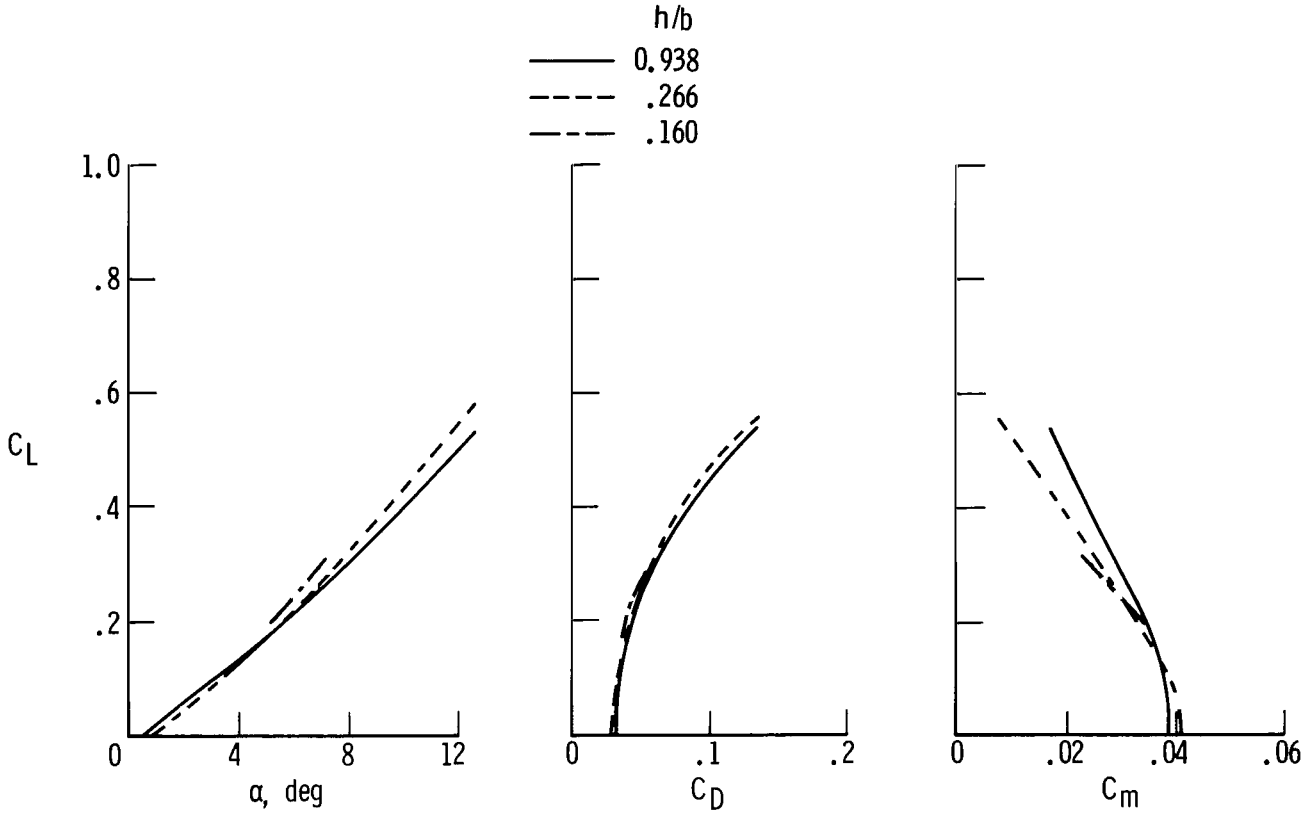

Figure 24. Basic wind-tunnel data (unpublished) for the XB-70 airplane.

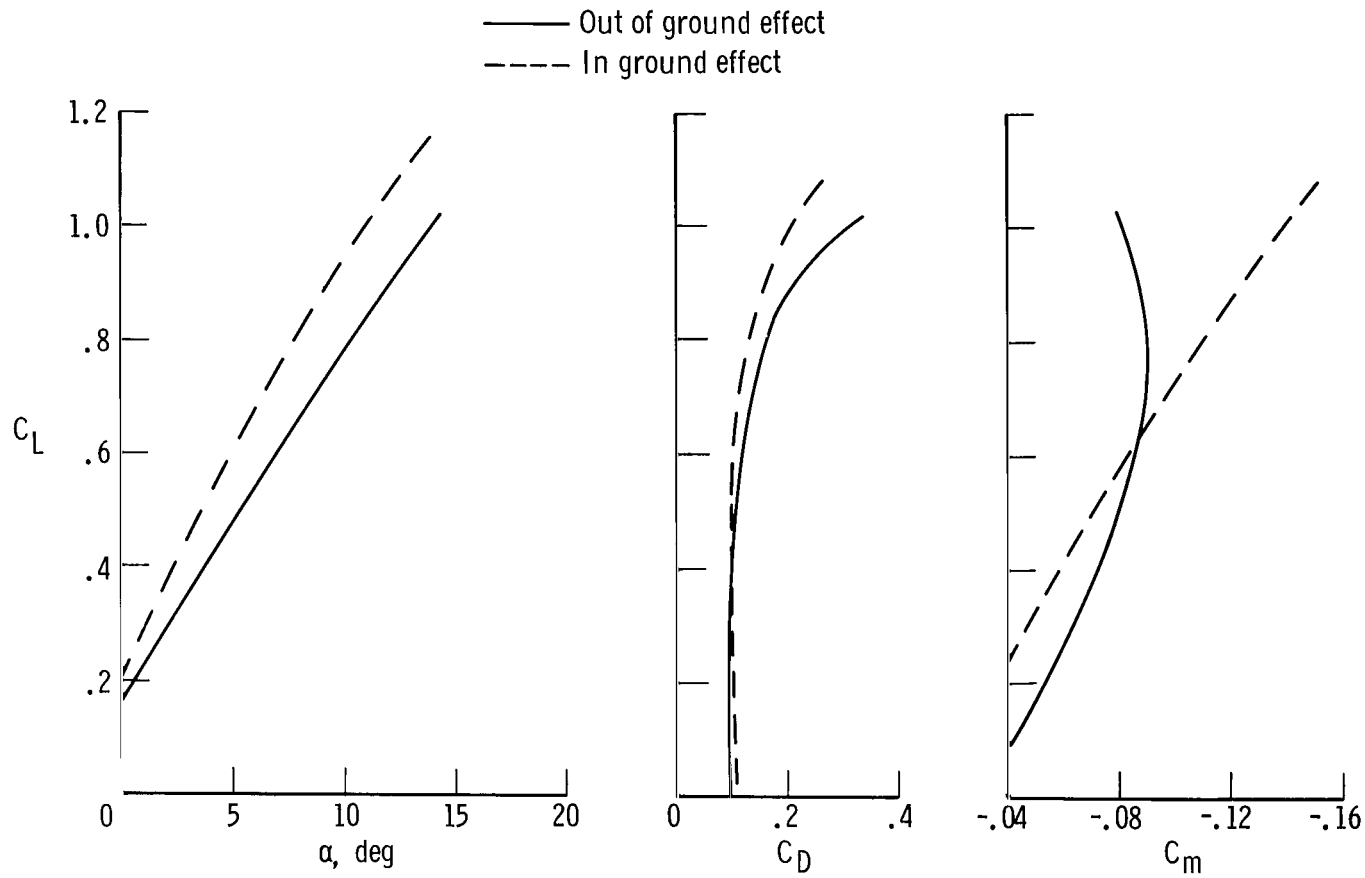

Figure 25. Basic wind-tunnel data (unpublished) for the F-104A airplane.

"The aeronautical and space activities of the United States shall be conducted so as to contribute . . . to the expansion of human knowledge of phenomena in the atmosphere and space. The Administration shall provide for the widest practicable and appropriate dissemination of information concerning its activities and the results thereof."

—NATIONAL AERONAUTICS AND SPACE ACT OF 1958

NASA SCIENTIFIC AND TECHNICAL PUBLICATIONS

TECHNICAL REPORTS: Scientific and technical information considered important, complete, and a lasting contribution to existing knowledge.

TECHNICAL NOTES: Information less broad in scope but nevertheless of importance as a contribution to existing knowledge.

TECHNICAL MEMORANDUMS: Information receiving limited distribution because of preliminary data, security classification, or other reasons.

CONTRACTOR REPORTS: Scientific and technical information generated under a NASA contract or grant and considered an important contribution to existing knowledge.

TECHNICAL TRANSLATIONS: Information published in a foreign language considered to merit NASA distribution in English.

SPECIAL PUBLICATIONS: Information derived from or of value to NASA activities. Publications include conference proceedings, monographs, data compilations, handbooks, sourcebooks, and special bibliographies.

TECHNOLOGY UTILIZATION PUBLICATIONS: Information on technology used by NASA that may be of particular interest in commercial and other non-aerospace applications. Publications include Tech Briefs, Technology Utilization Reports and Notes, and Technology Surveys.

Details on the availability of these publications may be obtained from:

SCIENTIFIC AND TECHNICAL INFORMATION DIVISION

NATIONAL AERONAUTICS AND SPACE ADMINISTRATION

Washington, D.C. 20546